NIH Public Access
Author Manuscript
Toxicol Appl Pharmacol. Author manuscript; available in PMC 2012 October 15.

Published in final edited form as:
Toxicol Appl Pharmacol. 2011 October 15; 256(2): 122–135. doi:10.1016/j.taap.2011.07.019.

Nrf2 protects against 2,3,7,8-tetrachlorodibenzo-*p*-dioxin (TCDD)-induced oxidative injury and steatohepatitis

Hong Lu[a,*], **Wei Cui**[b], and **Curtis D. Klaassen**[a]

[a]Department of Pharmacology, Toxicology & Therapeutics, University of Kansas Medical Center, Kansas City, Kansas 66160

[b]Department of Pathology and Laboratory Medicine, University of Kansas Medical Center, Kansas City, Kansas 66160

Abstract

Previous studies demonstrate that Nrf2, a master regulator of antioxidative responses, is essential in mediating induction of many antioxidative enzymes by acute activation of the AhR. However, the role of Nrf2 in protecting against oxidative stress and DNA damage induced by sustained activation of the AhR remains unknown and was investigated herein. Tissue and blood samples were collected from wild-type (WT) and Nrf2-null mice 21 days after administration of a low-toxic dose (10 μg/kg ip) of TCDD. Only Nrf2-null mice lost body weight after TCDD treatment; however, blood levels of ALT were not markedly changed in either genotype, indicating a lack of extensive necrosis. Compared to livers of TCDD-treated WT mice, livers of TCDD-treated Nrf2-null mice had: 1) degenerated hepatocytes, lobular inflammation, marked fat accumulation, and higher mRNA expression of inflammatory and fibrotic genes; 2) depletion of glutathione, elevation in lipid peroxidation and marker of DNA damage; 3) attenuated induction of phase-II enzymes Nqo1, Gsta1/2, and Ugt2b35 mRNAs, but higher induction of cytoprotective Ho-1, Prdx1, Trxr1, Gclc, and Epxh1 mRNAs; 4) higher mRNA expression of Fgf21 and triglyceride-synthesis genes, but down-regulation of bile-acid-synthesis genes and cholesterol-efflux transporters; and 5) trend of induction/activation of c-jun and NF-kB. Additionally, TCDD-treated Nrf2-null mice had impaired adipogenesis in white adipose tissue. In conclusion, Nrf2 protects livers of mice against oxidative stress, DNA damage, and steatohepatitis induced by TCDD-mediated sustained activation of the AhR. The aggravated hepatosteatosis in TCDD-treated Nrf2-null mice is due to increased lipogenesis in liver and impaired lipogenesis in white adipose tissue.

Keywords

AhR; Nrf2; knockout; TCDD; sustained activation; oxidative stress; steatohepatitis

© 2011 Elsevier Inc. All rights reserved.

Address correspondence to: Hong Lu, Ph.D., 3901 Rainbow Blvd., Kansas City, KS 66160. Tel: 913-878-9197; Fax: 913-588-7501; hlu@kumc.edu.

Publisher's Disclaimer: This is a PDF file of an unedited manuscript that has been accepted for publication. As a service to our customers we are providing this early version of the manuscript. The manuscript will undergo copyediting, typesetting, and review of the resulting proof before it is published in its final citable form. Please note that during the production process errors may be discovered which could affect the content, and all legal disclaimers that apply to the journal pertain.

Conflict of interest statement
There are no conflicts of interest.

NIH-PA Author Manuscript
NIH-PA Author Manuscript
NIH-PA Author Manuscript

NIH-PA Author Manuscript

NIH-PA Author Manuscript

NIH-PA Author Manuscript

Introduction

Polychlorinated dibenzo-*p*-dioxins are persistent environmental pollutants. The most potent congener, 2,3,7,8-tetrachlorodibenzo-*p*-dioxin (TCDD), acting through aryl hydrocarbon receptor (AhR)-mediated signaling pathways, produces various toxic and biochemical effects, such as reproductive and developmental defects, immunotoxicity, liver damage, wasting syndrome, and cancer at higher doses. There is consistency between humans and rodents in the target organs affected by dioxins (liver, oral cavity, cardiovascular system, immune system, thyroid, pancreas, and lung) (Yoshizawa *et al.*, 2007).

TCDD is classified as a non-genotoxic carcinogen because it is not mutagenic in bacteria or other *in vitro* assay systems. Induction of Cyp1a1, via binding of the AhR to the dioxin response element (DRE) in the Cyp1a1 gene, is a major cause of oxidative stress and wasting syndrome after dioxin exposure (Morel *et al.*, 1999; Uno *et al.*, 2004; Kopf *et al.*, 2010). Treatment of C57BL/6 mice with TCDD (15 μg/kg, ip) increases mitochondrial reactive oxygen species (ROS), which is dependent on the AhR; however, this low-toxic dose of TCDD also increases reduced glutathione (GSH) in liver mitochondria (Senft *et al.*, 2002). The protection against ROS-induced oxidative injury has been ascribed to the AhR-mediated induction of cytoprotective genes, such as NAD(P)H:quinone oxidoreductase 1 (Nqo1), glutathione *S*-transferases (Gsts), and UDP-glucuronosyltransferases (Ugts) (Nebert *et al.*, 2000).

Although the AhR is often regarded as the key transcription factor that mediates alteration of gene expression by TCDD, the nuclear factor erythroid 2 related factor 2 (Nrf2) is activated by TCDD as well, and in turn, Nrf2 regulates a battery of cytoprotective genes (Yeager *et al.*, 2009). AhR can induce Nrf2 mRNA expression via binding to DRE-like elements in the mouse Nrf2 promoter (Miao *et al.*, 2005), and the induction of Nqo1 by TCDD is dependent on both AhR and Nrf2 in cells (Ma *et al.*, 2004). A previous study illustrated that TCDD-induction of many of the cytoprotective genes, namely Nqo1, Gsts, and Ugts, is lost in Nrf2-null mice after TCDD treatment (Yeager *et al.*, 2009). However, it remains unknown whether Nrf2 deficiency aggravates AhR-induced oxidative stress and liver injury, particularly the risk of liver cancer.

The duration of AhR activation, namely transient versus sustained activation, has been suggested to be critical in determining the beneficial versus toxic effects of TCDD and other AhR ligands (Mitchell and Elferink, 2009). Interestingly, high-affinity endogenous ligands for human AhR, such as 2-(1'H-indole-3'-carbonyl)-thiazole-4-carboxylic acid methyl ester (ITE), kynurenic acid, and indoxyl-3-sulfate (I3S) (Henry *et al.*, 2006; DiNatale *et al.*, 2010; Schroeder *et al.*, 2010) were identified recently. Although TCDD and the endogenous AhR ligand ITE elicit the same immediate changes in gene expression in mouse lung fibroblasts, only the long-lived TCDD induces toxicity *in vivo* (Henry *et al.*, 2010). In contrast, the endogenous AhR ligand I3S accumulates to high micromolar concentrations in blood of kidney dialysis patients, suggesting that prolonged activation of the AhR by I3S may contribute to toxicity observed in kidney dialysis patients (Barreto *et al.*, 2009). Therefore, it is essential to understand the mechanism of toxicity induced by sustained activation of AhR by environmental and endogenous chemicals.

The toxicological effects of TCDD are highly dose- and time-dependent. TCDD at high doses causes injury to various tissues, including body wasting, hepatomegaly, thymic atrophy, and immune suppression. In our pilot time-course and dose-response study of the effects of TCDD on hepatic gene expression and toxicity in adult male C57BL/6 mice, a bolus TCDD dose of 10 μg/kg (ip) induced hepatic expression of AhR- and Nrf2-target genes without any effect on body weight, indicating that 10 μg/kg is a low-toxic dose of

NIH-PA Author Manuscript

NIH-PA Author Manuscript

NIH-PA Author Manuscript

TCDD in adult male C57BL/6 mice. TCDD is predominantly sequestered by liver after a bolus dose of 15 μg/kg in male C57BL/6 mice (Pegram *et al.*, 1995), and TCDD has a long half-life of 13.5 d in mouse liver (Manara *et al.*, 1982). Moreover, adult male mice treated with high doses of TCDD appear relatively healthy before 18 d after TCDD treatment, but their health deteriorate thereafter (Uno *et al.*, 2004). Therefore, in the present study, hepatic gene expression and pathophysiology as well as blood chemistry in wild-type (WT) and Nrf2-null mice were determined 21 d after administration of a bolus low-toxic dose of TCDD (10 μg/kg ip) to investigate the role of Nrf2 in protecting the liver against oxidative stress, DNA damage, and steatohepatitis induced by TCDD-mediated sustained activation of the AhR.

MATERIALS AND METHODS

Materials

TCDD was a gift from Dr. Karl Rozman (University of Kansas Medical Center, Kansas City, KS). All other materials, unless otherwise specified, were purchased from Sigma-Aldrich (St Louis, MO).

Treatment of animals

Nrf2-null mice have been previously described, and breeding pairs were obtained from Dr. Jefferson Chan (University of California Irvine, Irvine, CA) (Chan *et al.*, 1996). Nrf2-null mice were backcrossed with C57BL/6 mice (Charles River Laboratories, Inc., Wilmington, MA) and were determined to be > 99% congenic for the C57BL/6 background by Jackson Laboratories (Bar Harbor, ME). C57BL/6J WT mice were purchased from Jackson laboratories. All mice were fed Teklad Rodent Diet #8604 (Harlan Laboratories, Madison, WI) *ad libitum*, given free access to water, and were housed singly in an AAALAC-accredited animal care facility in temperature-, light-, and humidity-controlled rooms. Age-matched adult (8–9 weeks old) male WT C57BL/6 and Nrf2-null mice (n = 4–5 per group) were administered a single ip injection of either vehicle (corn oil, 10 ml/kg) or TCDD (10 μg/kg). Body weight and feed intake were recorded daily. Livers and epididymal white adipose tissues were collected 21 d after vehicle or TCDD, frozen in liquid nitrogen, and stored at −80°C. Trunk blood was collected and centrifuged to obtain serum. This study was approved by the University of Kansas Medical Center Institutional Animal Care and Use Committee.

RNA extraction

Total tissue RNA was extracted using RNA-Bee reagent (Tel-Test, Inc., Friendswood, TX) according to the manufacturer's protocol. Each RNA pellet was redissolved in 0.2 ml of diethyl pyrocarbonate-treated water. RNA concentrations were quantified by ultraviolet absorbance at 260 nm.

Determination of mRNAs with branched DNA (bDNA) signal amplification assay

mRNAs of genes expressed in livers (except genes in Figure 6A) were quantified using Quantigene® branched DNA (bDNA) signal amplification kit (Panomics/Affymetrix, Fremont, CA) with modifications (Hartley and Klaassen, 2000). The sequences of the bDNA probes for most of these drug-processing and nuclear-receptor genes have been reported previously (Buckley and Klaassen, 2007; Knight *et al.*, 2007; Zhang *et al.*, 2010), whereas sequences of the bDNA probes for other genes are provided in Supplemental Table 1. Luminescence of samples in 96-well plates was determined with a Synergy 2 Microplate reader (BioTek Instruments, Inc., Winooski, VT) and reported as relative light units (RLU) per 5 μg total RNA.

NIH-PA Author Manuscript

NIH-PA Author Manuscript

NIH-PA Author Manuscript

Determination of mRNAs with real-time PCR

mRNAs of genes important in cholesterol metabolism in liver and genes involved in adipogenesis in white adipose tissue were quantified by SYBR® Green real-time PCR. The PCR amplification reactions were carried out in an ABI Prism 7900 sequence detection system (Applied Biosystems). Primers of these genes are listed in Supplemental Table 2. The amount of mRNA was calculated using the comparative CT method, which determines the amount of target normalized to an endogenous reference, β-actin, with values of wild-type control set as 1.0.

Determination of GSH, catalase activity, xanthine oxidase (XO) activity, and lipid peroxidation in liver

Liver homogenates were used to quantify GSH by Ellman's reagent and a GSH standard curve (Ellman, 1959). Liver catalase activity was analyzed with Amplex® Red catalase assay kit (Invitrogen, Carlsbad, CA) using a standard curve of catalase. Briefly, to release catalase from peroxisomes, liver homogenates (in saline) were mixed with Triton X-100 (1%) and then further diluted 100 fold with 1X reaction buffer for the analysis of total catalase activity. Catalase activity was expressed as Units/mg protein. For determination of XO activity, liver samples were homogenized (1:20) in 0.1 M Tris-HCl buffer (pH 7.5) containing 1 mM EDTA. Liver homogenates were centrifuged at 10,000×g for 20 min at 4°C and the supernatants were assayed for XO activity using Amplex® Red Xanthine/ Xanthine Oxidase Assay Kit (MP-22182, Invitrogen) following the manufacturer's instructions. XO activity was determined by comparing the fluorescence of samples with that of XO standards and expressed as microunits/mg protein. Lipid peroxidation was determined by quantifying thiobarbituric acid reactive substances (TBARS). Briefly, about 25 mg of liver was dounce-homogenized in 2 volumes of ice-cold PBS, and TBARS were determined with the OXltek TBARS kit (ZeptoMetrix, Buffalo, NY). Liver homogenates and malondialdehyde (MDA) standards were incubated with sodium dodecyl sulfate and thiobarbituric acid at 95°C for 1 h. After incubation, samples were cooled on ice and centrifuged at 1,800 *g* for 15 min. Supernatants (200 μl) were transferred to a 96-well plate and read at 532 nm. Lipid peroxidation was expressed as nmol of MDA equivalents per gram liver.

Determination of lipids in mouse liver

Sixty mg of frozen liver tissue were homogenized in 0.6 ml of buffer containing 18 mM Tris, pH 7.5, 300 mM mannitol, 50 mM EGTA, and 0.1 mM phenylmethylsulfonyl fluoride (Tanaka *et al*., 2008). Liver homogenates (500 μl) were mixed with 4 ml of chloroform:methanol (2:1) and incubated overnight at room temperature with occasional shaking. The next day, 1.0 ml of H_2O was added, vortexed, and centrifuged at 3000 *g* for 5 min. The lower lipid phase was collected and concentrated by vacuum. The lipid pellets were dissolved in a mixture of 270 μl of isopropanol and 30 μl of Triton X-100 to determine triglycerides (TG), total cholesterol (CHO), and nonesterified fatty acids (NEFA) using commercial analytical kits (Wako Chemicals USA, Inc., Richmond, VA).

Western blot determination of NF-kB p65 and phosphorylated histone H2AX (γ-H2AX) protein

Liver nuclear extracts were prepared with a nuclear extract kit (Marligen Biosciences, Inc., Rockville, MD). Protein levels of p65 and γ-H2AX (H2A.x phosphorylated at S139) were determined by Western blot. Briefly, protein samples were boiled for 2 min and loaded onto 10% SDS–PAGE gels. After electrophoresis, proteins were transferred to PVDF membranes and probed with a polyclonal p65 antibody (Ab7970, Abcam, Cambridge, MA), a monoclonal γ-H2AX antibody (2212-1, Epitomics, Inc., Burlingame, CA), or a polyclonal

NIH-PA Author Manuscript

NIH-PA Author Manuscript

NIH-PA Author Manuscript

histone H3 antibody (Ab1791, Abcam). Signals were visualized with a horseradish peroxidase-conjugated secondary antibody. Protein levels of NF-kB p65 were normalized to histone H3. Protein levels of NF-kB p65 and histone H3 were quantified using ImageJ software (Rasband, W.S., ImageJ, NIH, Bethesda, Maryland, USA, http://rsb.info.nih.gov/ij/, 1997–2009).

Determination of activities of caspase-3 (Casp3) and caspase-8 (Casp8)

Liver tissues were homogenized in a buffer containing 25 mM Hepes, 5 mM $MgCl_2$, 5 mM EDTA, 2 mM DTT, and 0.1% CHAPS (pH 7.5) in a ratio of 1:4 (wt/vol) (Zender *et al.*, 2003). Homogenates were centrifuged at 12,000 × *g* for 10 min (4°C). Total protein (100 μg) from the supernatants was used to determine activities of caspase-3 and caspase-8 using the chromogenic substrates, namely 200 μM Ac-DEVD-pNA (A2559, Sigma) and Ac-IETD-pNA (A9968, Sigma), respectively, in 100 mM sodium phosphate/10 mM Tris/100 mM DTT, pH 7.5. Absorbance at 405 nm was determined in a microplate reader after incubation at 37°C for 1 h. Specific activities of caspase-3 and caspase-8 (nmol of pNA formed/min/mg) were calculated using standards of *p*-nitroaniline (pNA).

Statistics

Data are presented as mean ± standard error (SE). Differences between various groups were determined by SigmaPlot for Windows Version 11.0 (Systat Software, Inc., San Jose, CA) using ANOVA followed by Duncan's *post-hoc* multiple comparisons, with significance set at $p \leq 0.05$.

RESULTS

Alteration in body weight, tissue weight, and blood chemistry in TCDD-treated Nrf2-null mice

Because TCDD induces oxidative stress and tissue injury with time, the feed intake and body weight in TCDD-treated mice was monitored for 21 d. TCDD-treated WT mice had a body weight gain similar to the vehicle-treated WT mice. In contrast, Nrf2-null mice had less of an increase in body weight than WT mice after vehicle (corn oil) treatment, and Nrf2-null mice lost body weight after TCDD treatment (Table 1). TCDD-treated Nrf2-null mice appeared to have much less abdominal white adipose tissue than vehicle-treated Nrf2-null mice and TCDD-treated WT mice. The weight loss in TCDD-treated Nrf2-null mice was not due to anorexia, because there was no decrease in feed intake in these two genotypes after TCDD treatment (data not shown). TCDD treatment increased the liver/body weight ratio (~20%) in both genotypes, but had no effect on kidney/body weight ratio in either genotype. TCDD treatment tended to decrease the spleen/body weight ratio in Nrf2-null mice ($p = 0.067$).

TCDD treatment slightly increased blood levels of ALT in WT mice, but not in Nrf2-null mice (Table 1). In contrast, blood levels of ALP were higher in both the vehicle- and TCDD-treated Nrf2-null mice than in WT controls, although TCDD treatment did not significantly increase ALP in either genotype. TCDD treatment decreased blood levels of cholesterol in both genotypes, but did not affect blood levels of triglycerides or NEFA (Table 1).

Liver histopathology in TCDD-treated Nrf2-null mice

Vehicle-treated WT and Nrf2-null mice demonstrated unremarkable morphology (Fig. 1A-1 to Fig. 1A-2). TCDD-treated WT mice showed scattered focal mixed inflammatory infiltration and no significant steatosis was observed (Fig. 1A-3). In contrast, TCDD-treated Nrf2-null mice showed significant liver injury involving perivenular hepatocytes (Fig.

NIH-PA Author Manuscript

NIH-PA Author Manuscript

NIH-PA Author Manuscript

1A-4). The hepatocytes were enlarged with ballooning degeneration (Fig. 1A-5). As shown in Fig. 1A-6, there was lobular inflammation composed of lymphocytes, neutrophils and histiocytes with occasional microgranulomas and lipogranulomas. Scattered apoptotic hepatocytes (Fig. 1A-7) accompanied by lobular inflammation were also seen. In addition, as shown in Fig. 1A-8, hepatocytes with microvesicular steatosis were present intermingled with hydropic hepatocytes. However, no confluent necrosis of hepatocytes was seen.

Because mice with constitutively active AhR develop fatty liver (Lee *et al.*, 2010), lipids in livers of TCDD-treated mice were examined. Nrf2-null mouse livers tended to have higher basal levels of triglycerides than WT livers (p=0.08) (Fig. 1B). Sustained activation of the AhR by TCDD increased hepatic triglycerides markedly in WT mice (321%), and even more in Nrf2-null mice (748%), resulting in 190% higher triglycerides in TCDD-treated Nrf2-null mice than in TCDD-treated WT mice. There was no difference in basal levels of cholesterol between the two genotypes. Hepatic cholesterol levels remained unchanged in TCDD-treated WT mice, but tripled in TCDD-treated Nrf2-null mice (Fig. 1B). In contrast, TCDD did not alter hepatic NEFA in either genotype (data not shown).

Alteration in hepatic mRNAs of inflammatory and fibrotic genes in TCDD-treated Nrf2-null mice

TCDD induced tumor necrosis factor alpha (Tnfα) moderately (62%) in WT mice, but markedly (286%) in Nrf2-null mice (Fig. 1C). Similarly, TCDD induced inter-cellular adhesion molecule 1 (Icam1), which promotes the extravasation of inflammatory cells, 104% in WT mice, but 613% in Nrf2-null mice. In contrast, TCDD induced cyclooxygenase-2 (Cox-2) only in Nrf2-null mice (144%). Nrf2-null mice had higher basal expression of collagen 1a1 (Col1a1), and higher Col1a1 mRNAs after TCDD treatment (Fig. 1C). Similarly, Nrf2-null mice had higher α-smooth muscle actin (α-Sma) mRNAs both before and after TCDD treatment, although TCDD did not induce α-Sma significantly in either genotype (Fig. 1C). In summary, Nrf2-null mice had markedly exacerbated steatohepatitis after TCDD treatment.

Alteration in hepatic enzymes directly involved in the generation and detoxification of ROS

TCDD treatment induced Cyp1a1 mRNA markedly and similarly in both genotypes (Fig. 2, Left panel). Oxidation of fatty acids by Cyp4a increases the production of ROS (Hardwick *et al.*, 2009). Cyp4a14 mRNAs were much higher in both vehicle- and TCDD-treated Nrf2-null mice than the corresponding WT mice. AhR-mediated induction of XO activities has been ascribed to the increase of oxidative stress by TCDD (Sugihara *et al.*, 2001). Surprisingly, vehicle-treated Nrf2-null mice had 61% lower XO activities than vehicle-treated WT mice (Fig. 2). TCDD moderately increased XO activities in livers of both WT (30%) and Nrf2-null (42%) mice, resulting in persistent 57% lower XO activities in Nrf2-null mice than WT mice (Fig. 2).

TCDD did not alter superoxide dismutase 1 (Sod1) or Sod2 mRNAs (data not shown) in either genotype. In contrast, catalase (Cat) mRNA was only decreased (32%) in TCDD-treated Nrf2-null mice (data not shown). Surprisingly, Nrf2-null mice had 146% higher total catalase activity in liver than WT mice; however, TCDD decreased catalase activity 64% in Nrf2-null mice, but not in WT mice (Fig. 2).

Alteration in hepatic mRNAs of classical Nrf2-target detoxification genes in TCDD-treated Nrf2-null mice

Similar to previous results (Yeager *et al.*, 2009), TCDD treatment induced WT and mutant Nrf2 mRNA in WT and Nrf2-null mice, respectively, to a similar degree (Fig. 2, right panel). Real-time PCR results confirmed that the exon5 of Nrf2 mRNA was absent in livers

NIH-PA Author Manuscript

NIH-PA Author Manuscript

NIH-PA Author Manuscript

(data not shown) and white adipose tissues of Nrf2-null mice. Many of the Nrf2-target genes encode important second-line antioxidative enzymes. Gsta1 and Gsta2 share very high similarities in mRNA sequence and expression pattern; the bDNA method determines the total amount of Gsta1 and Gsta2 (Gsta1/2). Nqo1 and Gsta1/2 mRNAs were much lower in vehicle-treated Nrf2-null mice, and the induction of Nqo1 and Gsta1/2 by TCDD was attenuated in Nrf2-null mice, resulting in 75% and 68% lower Nqo1 and Gsta1/2 mRNAs, respectively, in Nrf2-null mice than WT mice (Fig. 2). Similarly, Ugt2b35 mRNA was much lower in vehicle- and TCDD-treated Nrf2-null mice than in WT mice. Therefore, hepatic induction of these classical Nrf2-target phase-II enzymes by TCDD was largely abolished/attenuated in Nrf2-null mice.

In contrast, glutamate cysteine ligase catalytic subunit (Gclc) mRNA was only induced in TCDD-treated Nrf2-null mice, which still had lower Gclc mRNA than WT mice, due to much lower basal Gclc expression in Nrf2-null mice (Fig. 3). Nrf2-null mice also had much lower basal expression of microsomal epoxide hydrolase (Epxh1) and somewhat lower thioredoxin reductase 1 (Trxr1), but higher induction of these two genes by TCDD (176% for Epxh1 and 86% for Trxr1), resulting in similar expression of these two genes in TCDD-treated WT and Nrf2-null mice. In contrast, peroxiredoxin 1 (Prdx1 or Prx1) was induced by TCDD only in Nrf2-null mice, which had higher Prdx1 mRNAs than TCDD-treated WT mice (Fig. 3). Likewise, TCDD treatment induced heme oxygenase-1 (Ho-1) mRNA moderately (76%) in WT mice, but more markedly (291%) in Nrf2-null mice (Fig. 3).

Alteration in hepatic oxidative stress as well as markers of cell proliferation and apoptosis in TCDD-treated Nrf2-null mice

TCDD-treatment did not alter hepatic GSH levels in WT mice, but decreased them 50% in Nrf2-null mice (Fig. 4A). Similarly, TCDD treatment did not alter hepatic levels of MDA in WT mice, but increased them 572% in Nrf2-null mice, indicating high levels of oxidative stress and lipid peroxidation in these mice. Hepatic protein levels of γ-H2AX, a well-established biomarker of DNA damage caused by double-strand breaks (Kuo and Yang, 2008), were determined by Western blot (Fig. 4B). Hepatic γ-H2AX protein was undetectable in vehicle-treated WT mice, slightly elevated in vehicle-treated Nrf2-null mice and TCDD-treated WT mice, but was markedly increased in TCDD-treated Nrf2-null mice, suggesting that the markedly elevated oxidative stress in TCDD-treated Nrf2-null mice results in considerable DNA damage. In parallel, Fanconi anemia-associated nuclease 1 (Fan1), a recently identified key enzyme in DNA repair (Kee and D'Andrea, 2010), was induced by TCDD only in Nrf2-null mice (Fig. 4C). Topoisomerase 2a (Top2a) is a key enzyme in DNA repair and replication. TCDD treatment induced mRNAs of Top2a and mKi67, a proliferative marker, moderately in WT mice (~80%), but markedly (907% and 589%, respectively) in Nrf2-null mice (Fig. 4C). Additionally, ornithine decarboxylase 1 (Odc1) mRNA was induced slightly by TCDD only in Nrf2-null mice (Fig. 4C). TCDD treatment increased hepatic activities of caspase-3 and caspase-8 in WT mice (47% and 41%), but more in Nrf2-null mice (84% and 86%). Taken together, TCDD-treated Nrf2-null mice had marked oxidative injury, increased apoptosis, and cell proliferation in liver.

Alteration in hepatic mRNAs of transcription factors essential in cell proliferation, apoptosis, and energy metabolism

Interestingly, Nrf2-null mice had lower basal c-Jun mRNA. TCDD treatment down-regulated c-Jun in WT mice, but tended to induce c-Jun in Nrf2-null mice (Fig. 5). In contrast, TCDD induced the proto-oncogene c-Myc in both genotypes, but tended to induce c-Myc more in WT mice. Growth arrest and DNA damage induced gene-45-beta (Gadd45β) is a NF-kB target gene, which by inhibiting c-Jun N-terminal kinase (Jnk) overactivation, promotes the survival of hepatocytes during liver regeneration (Papa *et al.*, 2004; Papa *et al.*,

NIH-PA Author Manuscript

NIH-PA Author Manuscript

NIH-PA Author Manuscript

2008). TCDD induced Gadd45β mRNA only in Nrf2-null mice (195%). These data suggest that AP-1 and NF-kB are activated in TCDD-treated Nrf2-null mice. Peroxisome proliferator-activated receptor gamma coactivator-1 alpha (Pgc-1α) is critical in regulating energy metabolism. Interestingly, Pgc-1α mRNA was higher in vehicle-treated Nrf2-null mice than WT mice, and was down-regulated by TCDD only in Nrf2-null mice (Fig. 5). TCDD treatment induced p21 mRNA 254% in WT mice but 1008% in Nrf2-null mice, suggesting that the p53-p21 pathway is markedly activated in TCDD-treated Nrf2-null mice due to DNA damage. In contrast, mRNAs of CCAAT/enhancer binding protein homologous protein (Chop), an apoptotic transcription factor and marker of endoplasmic reticulum (ER) stress, remained unchanged in TCDD-treated mice (Fig. 5), suggesting a lack of marked ER stress response in both genotypes after TCDD treatment. Nuclear translocation of the NF-kB p65 subunit was determined by Western blot as an indicator of NF-kB activation. Interestingly, livers of Nrf2-null mice had lower basal levels of nuclear NF-kB than WT mice (Fig. 5B). Nuclear translocation of NF-kB tended to increase more in TCDD-treated Nrf2-null mice (86%) than in TCDD-treated WT mice (40%), resulting in similar levels of nuclear NF-kB in these two genotypes after TCDD treatment (Fig. 5B).

Alteration in hepatic mRNAs of genes involved in cholesterol metabolism in TCDD-treated Nrf2-null mice

TCDD did not alter hepatic mRNAs of genes essential in basolateral uptake and efflux of cholesterol, namely scavenger receptor class B type I and Abca1, respectively (data not shown). In contrast, Nrf2-null mouse livers had 40% lower basal expression of apolipoprotein B (Apob), which effluxes triglycerides and cholesterol to the blood. TCDD decreased Apob mRNA 40% in WT mice, and also tended to decrease Apob mRNA in Nrf2-null mice (Fig. 6A). ATP binding cassette g5 (Abcg5) and Abcg8 function as a heterodimer to efflux cholesterol into bile. Nrf2-null mice tended to have lower hepatic mRNA expression of Abcg5 than WT mice before and after TCDD treatment (data not shown). In contrast, TCDD did not alter Abcg8 mRNA in WT mice, but tended to decrease it in Nrf2-null mice, resulting in 55% lower Abcg8 mRNA in TCDD-treated Nrf2-null mice than TCDD-treated WT mice (Fig. 6A).

TCDD did not alter hepatic mRNAs of two genes essential in cholesterol synthesis, namely HMG-CoA synthase 1 and HMG-CoA reductase, in either genotype (data not shown). Synthesis of bile acids is essential for the elimination of cholesterol. Two pathways, namely classic and alternative pathways are responsible for the biosynthesis of bile acids from cholesterol. Cyp7a1 and Cyp8b1 are two key enzymes in the classic/neutral pathway of bile acid biosynthesis. TCDD treatment down-regulated Cyp7a1 about 70% in both genotypes (Fig. 6A). In contrast, TCDD tended to decrease Cyp8b1 mRNA in WT mice, whereas significantly decreased Cyp8b1 (76%) in Nrf2-null mice. Cyp27a1 and Cyp7b1 are two key enzymes in the alternative/acidic pathway of bile acid biosynthesis. TCDD did not alter Cyp27a1 mRNA in WT mice, but tended to decrease it in Nrf2-null mice, resulting in 41% lower Cyp27a1 mRNA in TCDD-treated Nrf2-null mice than TCDD-treated WT mice (Fig. 6A). Additionally, Nrf2-null mice had much lower hepatic mRNA expression of Cyp7b1 than WT mice before and after TCDD treatment, although TCDD did not significantly further down-regulate Cyp7b1 in Nrf2-null mice. Therefore, these data strongly indicate that a decrease in catabolism (via bile acid synthesis) and low biliary excretion (via Abcg5/g8) of cholesterol are responsible for the markedly elevated hepatic levels of cholesterol in TCDD-treated Nrf2-null mice.

NIH-PA Author Manuscript

NIH-PA Author Manuscript

NIH-PA Author Manuscript

Alteration in hepatic mRNAs of genes involved in fatty acid metabolism in TCDD-treated Nrf2-null mice

To elucidate the mechanism of the markedly exacerbated hepatosteatosis (Fig. 1B) in TCDD-treated Nrf2-null mice, hepatic mRNA expression of various genes important in the uptake, synthesis, and metabolism of lipids was determined (Fig. 6B). Fibroblast growth factor 21 (Fgf21) promotes lipolysis in adipocytes in fed mice (Hotta *et al.*, 2009). Interestingly, Nrf2-null mice had 320% higher basal levels of Fgf21 mRNAs. TCDD treatment induced Fgf21 3–4 fold in both genotypes, resulting in 254% higher Fgf21 mRNAs in TCDD-treated Nrf2-null mice than WT mice. Chylomicrons, produced in the intestine, transport dietary triglycerides to peripheral tissues and cholesterol to the liver. Lipoprotein lipase (Lpl) is a key enzyme that hydrolyzes triglycerides of circulating chylomicrons, and liver-specific overexpression of Lpl causes fatty liver (Kim *et al.*, 2001). The resultant new particle, called chylomicron remnants, are enriched in cholesteryl ester and are rapidly removed from the circulation by the liver via low-density lipoprotein receptor (Ldlr). TCDD induced Lpl mRNAs to a similar degree (~290%) in both genotypes (Fig. 6B). Cd36 and fatty acid binding protein 1 (Fabp1) are responsible for uptake of fatty acids into hepatocytes and intracellular transport of fatty acids, respectively (Weisiger, 2007; Lee *et al.*, 2010). TCDD treatment induced Cd36 305% and 385% in WT and Nrf2-null mice, respectively, but down-regulated Fabp1 only in WT mice (28%). In contrast, TCDD treatment had no effect on Ldlr mRNAs (data not shown).

Uncoupling protein 2 (Ucp2) promotes mitochondrial oxidation of fatty acids. TCDD induced Ucp2 in both genotypes (Fig. 6B). Compared to TCDD-treated WT mice, TCDD-treated Nrf2-null mice had much higher Cyp4a14 (Fig. 2) but similar carnitine palmitoyltransferase 1a and acyl CoA oxidase (data not shown), key enzymes involved in mitochondrial and peroxisomal oxidation of fatty acids. Therefore, the higher hepatic accumulation of triglycerides in Nrf2-null mice is unlikely due to decreased fatty acid oxidation.

TCDD treatment tended to decrease fatty acid synthase (Fasn) in both genotypes (data not shown), which is consistent with inhibition of *de novo* fatty acid synthesis in livers of rats treated with low-toxic doses of TCDD (Lakshman *et al.*, 1988; Lakshman *et al.*, 1989). Diacylglycerol *O*-acyltransferase 2 (Dgat2) is a key enzyme in triglyceride synthesis (Stone *et al.*, 2004). Nrf2-null mice had higher Dgat2 mRNA before and after TCDD treatment, which tended to decrease, but not significantly, Dgat2 mRNA. In summary, compared to TCDD-treated WT mice, TCDD-treated Nrf2-null mice had similar induction of genes involved in hepatic hydrolysis (Lpl) and uptake (Cd36) of lipids, but higher expression of genes involved in lipid hydrolysis (Fgf21) and triglyceride synthesis (Dgat2).

Alteration in mRNAs of genes involved in adipogenesis in epididymal white adipose tissue (WAT) in TCDD-treated Nrf2-null mice

It appears that the markedly higher hepatosteatosis in TCDD-treated Nrf2-null mice than TCDD-treated WT mice cannot be explained solely by the moderate differences in hepatic expression of genes involved in lipid metabolism (Fig. 6B). Recently, Nrf2 is shown to be essential in adipogenesis (Pi *et al.*, 2010). Because the slight weight loss in Nrf2-null mice was not due to a decrease in feed intake, we hypothesized that a defect in adipogenesis in TCDD-treated Nrf2-null mice and resultant shift of lipids from adipose tissue to liver contributes to the aggravated hepatosteatosis in these mice. Messenger RNA expression of genes essential for AhR and Nrf2 signaling as well as adipogenesis in WAT was determined by real-time PCR (Fig. 7). TCDD induced Cyp1a1 in WAT similarly in both genotypes, but to a much lower degree than in liver (Fig. 7). TCDD also increased Nrf2 mRNA (31%) and Nqo1 mRNA (214%) in WT mice, but not in Nrf2-null mice.

NIH-PA Author Manuscript

NIH-PA Author Manuscript

NIH-PA Author Manuscript

Transcription factors CCAAT/enhancer-binding protein α (Cebpa) and β (Cebpb) are master regulators of adipogenesis. TCDD increased Cebpa mRNA (155%) in WT mice, but not in Nrf2-null mice. In contrast, TCDD markedly induced Cebpb mRNA (747%) in Nrf2-null mice, but not in WT mice (Fig. 7). Interestingly, vehicle-treated Nrf2-null mice had a higher ratio of Cebpa to Cebpb in WAT; however, after TCDD treatment, the ratio of Cebpa to Cebpb tended to increase in WT mice ($p = 0.07$), but sharply decreased 76% in Nrf2-null mice, resulting in a 81% lower ratio of Cebpa to Cebpb in Nrf2-null mice than WT mice. Peroxisome proliferator-activated receptor γ (Pparγ), a master regulator of lipogenesis, was down-regulated (33%) by TCDD only in WAT of Nrf2-null mice (Fig. 7). TCDD induced Pgc-1α (739%) and a lipogenic transcription factor, sterol regulatory element-binding protein 1c (Srebp-1c) (72%) mRNAs in WT mice, but tended to decrease them in Nrf2-null mice, resulting in 91% and 48% lower Pgc-1α and Srebp-1c mRNAs in TCDD-treated Nrf2-null mice than TCDD-treated WT mice (Fig. 7).

Alterations of these lipogenic transcription factors suggest that lipogenesis was impaired in TCDD-treated Nrf2-null mice. Consistently, adipsin, an adipocyte-specific adipokine, was down-regulated 31% by TCDD in Nrf2-null mice (Fig. 7). Adiponectin, an adipocyte-enriched peptide hormone, was 39% lower in TCDD-treated Nrf2-null mice than TCDD-treated WT mice. Interestingly, WAT of Nrf2-null mice had higher basal expression of ATP citrate lyase (Acly), a key enzyme in acetyl-CoA synthesis. However, TCDD induced Acly 153% in WT mice, but tended to down-regulate it in Nrf2-null mice, resulting in a trend of lower expression of Acly in TCDD-treated Nrf2-null mice. TCDD also induced Fasn in WT mice, but not in Nrf2-null mice. Stearoyl-Coenzyme A desaturase 1 (Scd1) is a key enzyme in fatty acid synthesis. TCDD tended to induce Scd1 in WT mice but down-regulate it in Nrf2-null mice, resulting in a 15% lower expression of Scd1 in TCDD-treated Nrf2-null mice than TCDD-treated WT mice (Fig. 7).

Discussion

The present data demonstrate that 21 d after administration of a low-toxic dose of TCDD (10 μg/kg), WT mice have induction of Nrf2 and certain Nrf2-target genes, hepatosteatosis, but minimum oxidative injury (as indicated by the maintenance of GSH, lack of elevation in lipid peroxidation, and minimal DNA damage). In contrast, TCDD-treated Nrf2-null mice have markedly elevated oxidative stress, DNA damage, and steatohepatitis. TCDD causes differential expression of lipogenic genes in liver and WAT of WT and Nrf2-null mice. The TCDD-induction of certain classical Nrf2-target phase-II enzymes is abolished/attenuated in Nrf2-null mice, whereas certain other Nrf2-target cytoprotective genes are induced more in TCDD-treated Nrf2-null mice, which may prevent overt necrotic cell death in these mice.

TCDD is classified as a non-genotoxic carcinogen, because it is not mutagenic in either bacteria or most *in vitro* assay systems. TCDD is the most potent liver tumor promoter in rodents, and constitutively-active AhR markedly promotes liver cancer in mice (Moennikes *et al.*, 2004). In the present study, TCDD-treated WT mice have increased expression of the proliferation markers mKi67 and Top2a, as well as induction of proinflammatory genes Tnfα and Icam1, which is consistent with the tumor-promoting characteristic of TCDD. However, TCDD-treated WT mice have minimal DNA damage and liver injury, which is consistent with a lack of tumor-initiating effects in liver by lower doses of TCDD in WT mice.

Oxidative DNA damage is closely associated with TCDD-induced liver cancer (Knerr and Schrenk, 2006). AhR-mediated induction of Cyp1a1 is a major cause of the increase in oxidative stress and liver injury after dioxin exposure (Morel *et al.*, 1999; Uno *et al.*, 2004). Oxidation of fatty acids by Cyp4a increases the production of ROS (Hardwick *et al.*, 2009).

NIH-PA Author Manuscript

NIH-PA Author Manuscript

NIH-PA Author Manuscript

The similar induction of Cyp1a1 and markedly higher expression of Cyp4a14 in TCDD-treated Nrf2-null mice likely causes a higher production of ROS. In contrast, Nrf2-null mice have lower antioxidative capacity, evidenced by the lower basal expression of antioxidative enzymes, such as Gclc, Nqo1, Epxh1, and Gsta1/2. Catalase is essential in the detoxification of hydrogen peroxide. The mechanism of down-regulation of catalase in TCDD-treated Nrf2-null mice remains unknown. Interestingly, prolonged oxidative stress by hydrogen peroxide down-regulates catalase via hypermethylation of its promoter in hepatoma cells (Min *et al.*, 2010). In TCDD-treated Nrf2-null mice, the marked imbalance between the production and detoxification of ROS results in depletion of GSH, marked oxidative stress, and DNA damage (Fig. 8).

The mechanism of novel finding of lower XO activities in vehicle- and TCDD-treated Nrf2-null mice than WT mice remains unknown. Consistent with literature (Sugihara *et al.*, 2001), TCDD increases XO activities in livers of both WT and Nrf2-null mice. Hepatic XO activity is decreased in rats fed low-protein diet or purified diet and during liver carcinogenesis induced by p-dimethylaminoazobenzene (Westerfeld *et al.*, 1950; Westerfeld and Richert, 1951). Interestingly, the low protein diets are characterized by fatty infiltration and hydropic degeneration of liver (Westerfeld *et al.*, 1950), which is similar to the pathological changes observed in TCDD-treated Nrf2-null mice (Fig. 1). Additionally, reactive nitrogen species peroxynitrite ($ONOO^-$) markedly inhibits XO activity via oxidative disruption of the molybdenum catalytic site (Lee *et al.*, 2000). The potential contribution of protein imbalance and peroxynitrite to decreased XO activities in Nrf2-null mice warrant further investigation.

The induction of phase-II enzymes Nqo1, Gsta1/2, and Ugt2b35 by TCDD-mediated sustained activation of the AhR is abolished/attenuated in livers of Nrf2-null mice. This is consistent with a previous acute study that induction of Nrf2 and Nqo1 by TCDD is AhR-dependent, and these three phase-II enzymes are not induced in Nrf2-null mice 24 h after TCDD treatment (Yeager *et al.*, 2009).

The present data demonstrate that certain Nrf2-target cytoprotective genes are induced by TCDD to a surprisingly higher degree in Nrf2-null mice than WT mice. Nrf2 is activated by low levels of ROS to protect cells against oxidative stress. In contrast, an intermediate amount of ROS activates NF-kB and AP-1 to ameliorate oxidative stress and promote cell survival (Gloire *et al.*, 2006). The decreases in c-Jun mRNA and nuclear translocation of NF-kB p65 protein in unstressed Nrf2-null livers is consistent with a previous report that hepatic mRNA expression of c-Jun and p65 decreases in unstressed Nrf2-null livers (Yang *et al.*, 2005). Trxr1, a selenoprotein that catalyzes the reduction of disulfide in the active site of thioredoxin, which regulates the redox status of the cells, is induced by Tnfα, and Trxr1 activates NF-kB (Sakurai *et al.*, 2004). Trxr1 has been reported as a Nrf2-target gene (Sakurai *et al.*, 2005). The induction of Trxr1 by TCDD in Nrf2-null mice (Fig. 3) may be due to elevated Tnfa (Fig. 1). Induction of Ho-1 is a late event in TCDD-induced hepatotoxicity. Ho-1 can be up-regulated by Nrf2, AP-1, and NF-kB (Farombi and Surh, 2006); activation of Nrf2 alone is not sufficient to induce Ho-1 (Okawa *et al.*, 2006). The higher induction of Ho-1 in TCDD-treated Nrf2-null mice might be due to activation of AP-1 and/or NF-kB in these mice. The expression of Gclc is increased by GSH depletion with the activation of the Jun/AP-1 transcription factor (Tanaka *et al.*, 1998). Although the basal expression of Gclc and Epxh1 is decreased in Nrf2-null mice, Gclc and Epxh1 mRNAs are induced only in Nrf2-null mice after TCDD treatment, which might be due to activation of AP-1 and/or NF-kB, known transactivators of Gclc and Epxh1 (Fig. 8) (Lu, 2009).

Interestingly, in TCDD-treated Nrf2-null mice, despite the depletion of glutathione, marked elevation of lipid peroxidation and DNA damage, there does not appear to be marked necrosis of hepatocytes, as indicated by histopathological analysis and blood levels of ALT.

NIH-PA Author Manuscript

NIH-PA Author Manuscript

NIH-PA Author Manuscript

Gadd45β is critical in protecting against liver injury and promoting cell proliferation induced by activation of JNK during liver regeneration (Papa *et al.*, 2008). The strong induction of Gadd45β in TCDD-treated Nrf2-null mice may prevent cell death induced by overactivation of JNK, which otherwise causes death of hepatocytes during chronic oxidative stress (Singh *et al.*, 2009). Taken together, activation of AP-1 and NF-kB in TCDD-treated Nrf2-null mice is likely responsible for the induction of many Nrf2-target cytoprotective genes, which may prevent the necrotic death of hepatocytes in these mice (Fig. 8). However, activation of AP-1 and NF-kB enhances pro-inflammatory responses. In livers of TCDD-treated Nrf2-null mice, the sustained oxidative stress and DNA damage, exacerbated inflammation, increased cell proliferation, but insufficient apoptosis markedly increases the risk of carcinogenesis. Therefore, further long-term studies on whether Nrf2 deficiency increases TCDD-induced liver carcinogenesis are warranted.

The present data demonstrate that Nrf2 deficiency markedly aggravate TCDD-induced hepatosteatosis. Dioxin exposure is associated with increased prevalence of fatty liver in humans (Lee *et al.*, 2006). Sustained activation of AhR by high doses of TCDD causes fatty liver and weight loss in rodents. The hepatosteatosis in TCDD-treated WT mice is consistent with a recent report that constitutively activated AhR causes fatty liver, at least partially via induction of Cd36 and decrease in peroxisomal β-oxidation of fatty acids (Lee *et al.*, 2010). When fed a high-fat diet, Nrf2-null mice have higher expression of lipid uptake and synthesis genes (Tanaka *et al.*, 2008). Moreover, when fed a methionine- and choline-deficient (MCD) diet, Nrf2-null mice have more severe hepatosteatosis (Chowdhry *et al.*, 2010; Sugimoto *et al.*, 2010; Zhang *et al.*, 2010). In the present study, when fed a normal chow, TCDD-treated Nrf2-null mice have approximately 3 times the triglyceride concentration in livers of WT mice. Sustained activation of AhR by TCDD induces a group of genes that function in the mobilization and uptake of lipids (Fig. 6). However, TCDD-treated WT and Nrf2-null mice have similar induction of lipogenic genes in liver, suggesting that the aggravated hepatosteatosis due to Nrf2 deficiency cannot be solely explained by differences in hepatic lipid metabolism between TCDD-treated WT and Nrf2-null mice.

The differential effects of TCDD on WAT of WT and Nrf2-null mice are intriguing. Both AhR and Nrf2 signaling are functional in WAT (Yoshinari *et al.*, 2006). Although higher doses of TCDD cause weight loss, lower doses of TCDD slightly increase body weight in rodents (Croutch *et al.*, 2005). Moreover, intrauterine exposure to dioxin-like compounds and PCBs is associated with higher body mass index (BMI) during early childhood (Verhulst *et al.*, 2009). TCDD (at 10 μg/kg) moderately induces AhR target genes Cyp1a1 and Nrf2 in WAT (Fig. 7), suggesting a moderate magnitude of activation of AhR in WAT by this dose of TCDD. Very interestingly, TCDD induces lipogenic factors Cebpa, Pgc-1α, and Srebp-1c in WAT of WT mice, resulting in induction of key enzymes involved in lipogenesis, namely Acly and Fasn (Fig. 7). A previous study showed that TCDD dose-dependently induces mRNA expression of Cebpb, but down-regulates Cebpa in WAT of C57BL/6 mice up to 7 days after TCDD treatment (Liu *et al.*, 1998). During adipocyte differentiation, Cebpb is induced at an early stage, followed by induction of Cebpa and Pparγ. Both Cebpb and Cebpa are important for adipogenesis. A reduced ratio of Cebpa to Cebpb is associated with dedifferentiation of adipocytes by Tnfα (Ron *et al.*, 1992). It is proposed that a decreased ratio of Cebpa to Cebpb by TCDD impairs adipogenesis in mice with acute exposure to higher doses of TCDD (Liu *et al.*, 1998). Therefore, it is likely that exposure to higher doses of TCDD impairs adipogenesis through induction of Cebpb and decrease of the ratio of Cebpa to Cebpb, whereas prolonged exposure to lower doses of TCDD might promote adipogenesis through induction of Cebpa and Pgc-1α. In light of the increased BMI associated with exposure to low doses of AhR ligands in rodents and humans (Croutch *et al.*, 2005; Verhulst *et al.*, 2009), the role of AhR activation in lipogenesis in WAT and its impact on BMI warrant further investigation.

NIH-PA Author Manuscript

NIH-PA Author Manuscript

NIH-PA Author Manuscript

Adipose tissue is the primary site of lipid storage; impaired adipogenesis causes channeling of lipids to liver and resultant fatty liver. Adipose-specific knockout of Pparγ causes progressive loss of adipose tissue and hepatosteatosis, despite a lack of elevation in blood basal levels of triglycerides and NEFA (He *et al.*, 2003). Similarly, TCDD-treated WT and Nrf2-null mice have similar blood lipid profiles (Table 1), despite their marked differences in adipogenesis (Fig. 7). The impaired adipogenesis in TCDD-treated Nrf2-null mice likely contributes to both weight loss (Table 1) and aggravated hepatosteatosis (Fig. 1), as more fatty acids may be channeled to livers of these mice.

The present data reveal a novel role of Nrf2 in regulating the biosynthesis of bile acids (Fig. 6). Although some mice with Cyp7a1 deficiency have postnatal lethality, the survived Cyp7a1-null mice overcome bile acid deficiency through induction of Cyp7b1 and the alternative pathway of bile acid biosynthesis (Schwarz *et al.*, 1996). In TCDD-treated wild-type mice, only the classical pathway through Cyp7a1 was decreased. In contrast, in TCDD-treated Nrf2-null mice, the classical pathway (through Cyp7a1-Cyp8b1) was markedly decreased, and the alternative pathway (through Cyp27a1-Cyp7b1), which has a much lower basal levels in Nrf2-null mice, tended to be decreased. Therefore, in TCDD-treated Nrf2-null mice, both the classical and alternative pathways of bile acid biosynthesis are compromised, contributing to elevated cholesterol in livers of TCDD-treated Nrf2-null mice.

Sustained activation of AhR by TCDD (10 μg/kg) causes weight loss in Nrf2-null mice, but not in WT mice (Table 1). Interestingly, the weight loss in TCDD-treated Nrf2-null mice is not due to hypophagia. Pgc-1α plays a key role in regulating mitochondrial biogenesis, oxidative metabolism, and energy metabolism in various cells (Lin, 2009). The down-regulation of Pgc-1α by TCDD in Nrf2-null mice might be due to oxidative stress (Pirinen *et al.*, 2007). Therefore, the weight loss in TCDD-treated Nrf2-null mice might be due to a combined effect of impaired adipogenesis and disrupted hepatic energy metabolism because of mitochondrial dysfunction (by severe oxidative stress), which warrants further investigation.

In conclusion, the present data demonstrate clearly the key role of Nrf2 in protecting the mouse liver against oxidative stress, DNA damage, and steatohepatitis induced by TCDD-mediated sustained activation of AhR. Activation of stress signaling pathways (e.g. AP-1 and NF-kB) in TCDD-treated Nrf2-null mice is likely responsible for hepatic induction of certain cytoprotective genes and aggravated inflammatory responses. Moreover, the present study discovers a novel role of Nrf2 in protection against TCDD-mediated impairment of adipogenesis which contributes to weight loss and hepatosteatosis in TCDD-treated Nrf2-null mice. Future studies on the time-course changes in gene expression and physiological function in liver and WAT of TCDD-treated Nrf2-null mice will further our understanding of how the interplay of AhR-Nrf2 crosstalk between liver and adipose tissues influences steatohepatitis and liver fibrosis when the body is exposed to various environmental and endogenous AhR ligands.

Highlights

>TCDD causes hepatosteatosis and induction of Nrf2-target genes in wild-type mice.
>TCDD causes weight loss, oxidative injury, and steatohepatitis in Nrf2-null mice.
>Livers of TCDD-treated Nrf2-null mice have lower Nqo1, Gsta1/2, and Ugt2b35 mRNAs. > Livers of TCDD-treated Nrf2-null mice have lipogenic gene expression profiles. > White adipose tissues of TCDD-treated Nrf2-null mice have impaired adipogenesis.

NIH-PA Author Manuscript

NIH-PA Author Manuscript

NIH-PA Author Manuscript

Supplementary Material

Refer to Web version on PubMed Central for supplementary material.

Abbreviations

Ahr	aryl hydrocarbon receptor
Nrf2	nuclear factor erythroid 2 related factor 2
TCDD	2,3,7,8-tetrachlorodibenzo-*p*-dioxin
WT	wild-type
ALT	alanine aminotransferase
mKi-67	antigen identified by monoclonal antibody Ki-67
Top2a	topoisomerase 2-alpha
Cyp	cytochrome p450
Nqo1	NAD(P)H:quinone oxidoreductase 1
Gst	glutathione *S*-transferase
Ugt	UDP-glucuronosyltransferases
Ho-1	heme oxygenase-1
Prdx1	peroxiredoxin 1
Trxr1	thioredoxin reductase 1
Gclc	glutamate cysteine ligase catalytic subunit
Epxh1	microsomal epoxide hydrolase
Fgf21	fibroblast growth factor 21
Abcg8	ATP binding cassette g8
DRE	dioxin response element
ROS	reactive oxygen species
GSH	reduced glutathione
ITE	2-(1'H-indole-3'-carbonyl)-thiazole-4-carboxylic acid methyl ester
I3S	indoxyl-3-sulfate
bDNA	branched DNA
TBARS	thiobarbituric acid reactive substances
MDA	malondialdehyde
TG	triglycerides
CHO	cholesterol
NEFA	nonesterified fatty acids
γ-H2AX	phosphorylated histone H2AX
Casp3	caspase-3
Casp8	caspase-8
pNA	*p*-nitroaniline

NIH-PA Author Manuscript

NIH-PA Author Manuscript

NIH-PA Author Manuscript

Tnfα	tumor necrosis factor alpha
Icam1	inter-cellular adhesion molecule 1
Cox-2	cyclooxygenase-2
Col1a1	collagen 1a1
α-Sma	α-smooth muscle actin
XO	xanthine oxidase
Sod1	superoxide dismutase 1
Cat	catalase
Fan1	Fanconi anemia-associated nuclease 1
Odc1	ornithine decarboxylase 1
Gadd45β	growth arrest and DNA damage induced gene-45-beta
Jnk	c-Jun N-terminal kinase
Pgc-1α	peroxisome proliferator-activated receptor gamma coactivator-1 alpha
Chop	CCAAT/enhancer binding protein homologous protein
ER	endoplasmic reticulum
Apob	apolipoprotein B
Lpl	lipoprotein lipase
Ldlr	low-density lipoprotein receptor
Fabp1	fatty acid binding protein 1
Ucp2	uncoupling protein 2
Fasn	fatty acid synthase
Dgat2	diacylglycerol *O*-acyltransferase 2
WAT	white adipose tissue
Cebp	CCAAT/enhancer-binding protein
Pparγ	peroxisome proliferator-activated receptor γ
Srebp-1c	sterol regulatory element-binding protein 1c
Acly	ATP citrate lyase
Scd1	stearoyl-Coenzyme A desaturase 1

Acknowledgments

We thank Dr. Jefferson Chan (University of California Irvine, Irvine, CA) for providing breeding pairs of Nrf2-null mice, Dr. Karl K. Rozman for providing TCDD, Xiaohong (Lucy) Lei for technical assistance, and the postdoctoral fellows and graduate students in Dr. Klaassen's laboratory for critical review of the manuscript.

This work was supported in part by National Institutes of Health grants DK081461, CA143656, and RR021940.

NIH-PA Author Manuscript

NIH-PA Author Manuscript

NIH-PA Author Manuscript

References

Barreto FC, Barreto DV, Liabeuf S, Meert N, Glorieux G, Temmar M, Choukroun G, Vanholder R, Massy ZA. Serum indoxyl sulfate is associated with vascular disease and mortality in chronic kidney disease patients. Clin J Am Soc Nephrol. 2009; 4:1551–1558. [PubMed: 19696217]

Buckley DB, Klaassen CD. Tissue- and gender-specific mRNA expression of UDP-glucuronosyltransferases (UGTs) in mice. Drug metabolism and disposition: the biological fate of chemicals. 2007; 35:121–127. [PubMed: 17050650]

Chan K, Lu R, Chang JC, Kan YW. NRF2, a member of the NFE2 family of transcription factors, is not essential for murine erythropoiesis, growth, and development. Proceedings of the National Academy of Sciences of the United States of America. 1996; 93:13943–13948. [PubMed: 8943040]

Chowdhry S, Nazmy MH, Meakin PJ, Dinkova-Kostova AT, Walsh SV, Tsujita T, Dillon JF, Ashford ML, Hayes JD. Loss of Nrf2 markedly exacerbates nonalcoholic steatohepatitis. Free radical biology & medicine. 2010; 48:357–371. [PubMed: 19914374]

Croutch CR, Lebofsky M, Schramm KW, Terranova PF, Rozman KK. 2,3,7,8-Tetrachlorodibenzo-p-dioxin (TCDD) and 1,2,3,4,7,8-hexachlorodibenzo-p-dioxin (HxCDD) alter body weight by decreasing insulin-like growth factor I (IGF-I) signaling. Toxicol Sci. 2005; 85:560–571. [PubMed: 15703265]

DiNatale BC, Murray IA, Schroeder JC, Flaveny CA, Lahoti TS, Laurenzana EM, Omiecinski CJ, Perdew GH. Kynurenic acid is a potent endogenous aryl hydrocarbon receptor ligand that synergistically induces interleukin-6 in the presence of inflammatory signaling. Toxicol Sci. 2010; 115:89–97. [PubMed: 20106948]

Ellman GL. Tissue sulfhydryl groups. Archives of biochemistry and biophysics. 1959; 82:70–77. [PubMed: 13650640]

Farombi EO, Surh YJ. Heme oxygenase-1 as a potential therapeutic target for hepatoprotection. Journal of biochemistry and molecular biology. 2006; 39:479–491. [PubMed: 17002867]

Gloire G, Legrand-Poels S, Piette J. NF-kappaB activation by reactive oxygen species: fifteen years later. Biochem Pharmacol. 2006; 72:1493–1505. [PubMed: 16723122]

Hardwick JP, Osei-Hyiaman D, Wiland H, Abdelmegeed MA, Song BJ. PPAR/RXR regulation of fatty acid metabolism and fatty acid omega-hydroxylase (CYP4) isozymes: Implications for prevention of lipotoxicity in fatty liver disease. PPAR research. 2009; 2009:952734. [PubMed: 20300478]

Hartley DP, Klaassen CD. Detection of chemical-induced differential expression of rat hepatic cytochrome P450 mRNA transcripts using branched DNA signal amplification technology. Drug metabolism and disposition: the biological fate of chemicals. 2000; 28:608–616. [PubMed: 10772642]

He W, Barak Y, Hevener A, Olson P, Liao D, Le J, Nelson M, Ong E, Olefsky JM, Evans RM. Adipose-specific peroxisome proliferator-activated receptor gamma knockout causes insulin resistance in fat and liver but not in muscle. Proceedings of the National Academy of Sciences of the United States of America. 2003; 100:15712–15717. [PubMed: 14660788]

Henry EC, Bemis JC, Henry O, Kende AS, Gasiewicz TA. A potential endogenous ligand for the aryl hydrocarbon receptor has potent agonist activity in vitro and in vivo. Archives of biochemistry and biophysics. 2006; 450:67–77. [PubMed: 16545771]

Henry EC, Welle SL, Gasiewicz TA. TCDD and a putative endogenous AhR ligand, ITE, elicit the same immediate changes in gene expression in mouse lung fibroblasts. Toxicol Sci. 2010; 114:90–100. [PubMed: 19933214]

Hotta Y, Nakamura H, Konishi M, Murata Y, Takagi H, Matsumura S, Inoue K, Fushiki T, Itoh N. Fibroblast growth factor 21 regulates lipolysis in white adipose tissue but is not required for ketogenesis and triglyceride clearance in liver. Endocrinology. 2009; 150:4625–4633. [PubMed: 19589869]

Kee Y, D'Andrea AD. Expanded roles of the Fanconi anemia pathway in preserving genomic stability. Genes & development. 2010; 24:1680–1694. [PubMed: 20713514]

Kim JK, Fillmore JJ, Chen Y, Yu C, Moore IK, Pypaert M, Lutz EP, Kako Y, Velez-Carrasco W, Goldberg IJ, Breslow JL, Shulman GI. Tissue-specific overexpression of lipoprotein lipase causes

NIH-PA Author Manuscript NIH-PA Author Manuscript NIH-PA Author Manuscript

tissue-specific insulin resistance. Proceedings of the National Academy of Sciences of the United States of America. 2001; 98:7522–7527. [PubMed: 11390966]

Knerr S, Schrenk D. Carcinogenicity of 2,3,7,8-tetrachlorodibenzo-p-dioxin in experimental models. Mol Nutr Food Res. 2006; 50:897–907. [PubMed: 16977593]

Knight TR, Choudhuri S, Klaassen CD. Constitutive mRNA expression of various glutathione S-transferase isoforms in different tissues of mice. Toxicol Sci. 2007; 100:513–524. [PubMed: 17890767]

Kopf PG, Scott JA, Agbor LN, Boberg JR, Elased KM, Huwe JK, Walker MK. Cytochrome P4501A1 is required for vascular dysfunction and hypertension induced by 2,3,7,8-tetrachlorodibenzo-p-dioxin. Toxicol Sci. 2010; 117:537–546. [PubMed: 20634294]

Kuo LJ, Yang LX. Gamma-H2AX - a novel biomarker for DNA double-strand breaks. In Vivo. 2008; 22:305–309. [PubMed: 18610740]

Lakshman MR, Campbell BS, Chirtel SJ, Ekarohita N. Effects of 2,3,7,8-tetrachlorodibenzo-p-dioxin (TCDD) on de novo fatty acid and cholesterol synthesis in the rat. Lipids. 1988; 23:904–906. [PubMed: 3185127]

Lakshman MR, Chirtel SJ, Chambers LL, Coutlakis PJ. Effects of 2,3,7,8-tetrachlorodibenzo-p-dioxin on lipid synthesis and lipogenic enzymes in the rat. The Journal of pharmacology and experimental therapeutics. 1989; 248:62–66. [PubMed: 2913289]

Lee CC, Yao YJ, Chen HL, Guo YL, Su HJ. Fatty liver and hepatic function for residents with markedly high serum PCDD/Fs levels in Taiwan. J Toxicol Environ Health A. 2006; 69:367–380. [PubMed: 16455615]

Lee CI, Liu X, Zweier JL. Regulation of xanthine oxidase by nitric oxide and peroxynitrite. The Journal of biological chemistry. 2000; 275:9369–9376. [PubMed: 10734080]

Lee JH, Wada T, Febbraio M, He J, Matsubara T, Lee MJ, Gonzalez FJ, Xie W. A novel role for the dioxin receptor in fatty acid metabolism and hepatic steatosis. Gastroenterology. 2010; 139:653–663. [PubMed: 20303349]

Lin JD. Minireview: the PGC-1 coactivator networks: chromatin-remodeling and mitochondrial energy metabolism. Molecular endocrinology (Baltimore, Md. 2009; 23:2–10.

Liu PC, Dunlap DY, Matsumura F. Suppression of C/EBPalpha and induction of C/EBPbeta by 2,3,7,8-tetrachlorodibenzo-p-dioxin in mouse adipose tissue and liver. Biochem Pharmacol. 1998; 55:1647–1655. [PubMed: 9634001]

Lu SC. Regulation of glutathione synthesis. Mol Aspects Med. 2009; 30:42–59. [PubMed: 18601945]

Ma Q, Kinneer K, Bi Y, Chan JY, Kan YW. Induction of murine NAD(P)H:quinone oxidoreductase by 2,3,7,8-tetrachlorodibenzo-p-dioxin requires the CNC (cap 'n' collar) basic leucine zipper transcription factor Nrf2 (nuclear factor erythroid 2-related factor 2): cross-interaction between AhR (aryl hydrocarbon receptor) and Nrf2 signal transduction. The Biochemical journal. 2004; 377:205–213. [PubMed: 14510636]

Manara L, Coccia P, Croci T. Persistent tissue levels of TCDD in the mouse and their reduction as related to prevention of toxicity. Drug metabolism reviews. 1982; 13:423–446. [PubMed: 7105970]

Miao W, Hu L, Scrivens PJ, Batist G. Transcriptional regulation of NF-E2 p45-related factor (NRF2) expression by the aryl hydrocarbon receptor-xenobiotic response element signaling pathway: direct cross-talk between phase I and II drug-metabolizing enzymes. The Journal of biological chemistry. 2005; 280:20340–20348. [PubMed: 15790560]

Min JY, Lim SO, Jung G. Downregulation of catalase by reactive oxygen species via hypermethylation of CpG island II on the catalase promoter. FEBS letters. 2010; 584:2427–2432. [PubMed: 20416298]

Mitchell KA, Elferink CJ. Timing is everything: consequences of transient and sustained AhR activity. Biochem Pharmacol. 2009; 77:947–956. [PubMed: 19027718]

Moennikes O, Loeppen S, Buchmann A, Andersson P, Ittrich C, Poellinger L, Schwarz M. A constitutively active dioxin/aryl hydrocarbon receptor promotes hepatocarcinogenesis in mice. Cancer research. 2004; 64:4707–4710. [PubMed: 15256435]

Morel Y, Mermod N, Barouki R. An autoregulatory loop controlling CYP1A1 gene expression: role of H(2)O(2) and NFI. Molecular and cellular biology. 1999; 19:6825–6832. [PubMed: 10490621]

NIH-PA Author Manuscript

NIH-PA Author Manuscript

NIH-PA Author Manuscript

Nebert DW, Roe AL, Dieter MZ, Solis WA, Yang Y, Dalton TP. Role of the aromatic hydrocarbon receptor and [Ah] gene battery in the oxidative stress response, cell cycle control, and apoptosis. Biochem Pharmacol. 2000; 59:65–85. [PubMed: 10605936]

Okawa H, Motohashi H, Kobayashi A, Aburatani H, Kensler TW, Yamamoto M. Hepatocyte-specific deletion of the keap1 gene activates Nrf2 and confers potent resistance against acute drug toxicity. Biochemical and biophysical research communications. 2006; 339:79–88. [PubMed: 16293230]

Papa S, Zazzeroni F, Bubici C, Jayawardena S, Alvarez K, Matsuda S, Nguyen DU, Pham CG, Nelsbach AH, Melis T, De Smaele E, Tang WJ, D'Adamio L, Franzoso G. Gadd45 beta mediates the NF-kappa B suppression of JNK signalling by targeting MKK7/JNKK2. Nature cell biology. 2004; 6:146–153.

Papa S, Zazzeroni F, Fu YX, Bubici C, Alvarez K, Dean K, Christiansen PA, Anders RA, Franzoso G. Gadd45beta promotes hepatocyte survival during liver regeneration in mice by modulating JNK signaling. The Journal of clinical investigation. 2008; 118:1911–1923. [PubMed: 18382767]

Pegram RA, Diliberto JJ, Moore TC, Gao P, Birnbaum LS. 2,3,7,8-Tetrachlorodibenzo-p-dioxin (TCDD) distribution and cytochrome P4501A induction in young adult and senescent male mice. Toxicology letters. 1995; 76:119–126. [PubMed: 7725343]

Pi J, Leung L, Xue P, Wang W, Hou Y, Liu D, Yehuda-Shnaidman E, Lee C, Lau J, Kurtz TW, Chan JY. Deficiency in the nuclear factor E2-related factor-2 transcription factor results in impaired adipogenesis and protects against diet-induced obesity. The Journal of biological chemistry. 2010; 285:9292–9300. [PubMed: 20089859]

Pirinen E, Kuulasmaa T, Pietila M, Heikkinen S, Tusa M, Itkonen P, Boman S, Skommer J, Virkamaki A, Hohtola E, Kettunen M, Fatrai S, Kansanen E, Koota S, Niiranen K, Parkkinen J, Levonen AL, Yla-Herttuala S, Hiltunen JK, Alhonen L, Smith U, Janne J, Laakso M. Enhanced polyamine catabolism alters homeostatic control of white adipose tissue mass, energy expenditure, and glucose metabolism. Molecular and cellular biology. 2007; 27:4953–4967. [PubMed: 17485446]

Ron D, Brasier AR, McGehee RE Jr, Habener JF. Tumor necrosis factor-induced reversal of adipocytic phenotype of 3T3-L1 cells is preceded by a loss of nuclear CCAAT/enhancer binding protein (C/EBP). The Journal of clinical investigation. 1992; 89:223–233. [PubMed: 1729273]

Sakurai A, Nishimoto M, Himeno S, Imura N, Tsujimoto M, Kunimoto M, Hara S. Transcriptional regulation of thioredoxin reductase 1 expression by cadmium in vascular endothelial cells: role of NF-E2-related factor-2. Journal of cellular physiology. 2005; 203:529–537. [PubMed: 15521073]

Sakurai A, Yuasa K, Shoji Y, Himeno S, Tsujimoto M, Kunimoto M, Imura N, Hara S. Overexpression of thioredoxin reductase 1 regulates NF-kappa B activation. Journal of cellular physiology. 2004; 198:22–30. [PubMed: 14584040]

Schroeder JC, Dinatale BC, Murray IA, Flaveny CA, Liu Q, Laurenzana EM, Lin JM, Strom SC, Omiecinski CJ, Amin S, Perdew GH. The uremic toxin 3-indoxyl sulfate is a potent endogenous agonist for the human aryl hydrocarbon receptor. Biochemistry. 2010; 49:393–400. [PubMed: 20000589]

Schwarz M, Lund EG, Setchell KD, Kayden HJ, Zerwekh JE, Bjorkhem I, Herz J, Russell DW. Disruption of cholesterol 7alpha-hydroxylase gene in mice. II. Bile acid deficiency is overcome by induction of oxysterol 7alpha-hydroxylase. The Journal of biological chemistry. 1996; 271:18024–18031. [PubMed: 8663430]

Senft AP, Dalton TP, Nebert DW, Genter MB, Puga A, Hutchinson RJ, Kerzee JK, Uno S, Shertzer HG. Mitochondrial reactive oxygen production is dependent on the aromatic hydrocarbon receptor. Free radical biology & medicine. 2002; 33:1268–1278. [PubMed: 12398935]

Singh R, Wang Y, Schattenberg JM, Xiang Y, Czaja MJ. Chronic oxidative stress sensitizes hepatocytes to death from 4-hydroxynonenal by JNK/c-Jun overactivation. Am J Physiol Gastrointest Liver Physiol. 2009; 297:G907–G917. [PubMed: 20501438]

Stone SJ, Myers HM, Watkins SM, Brown BE, Feingold KR, Elias PM, Farese RV Jr. Lipopenia and skin barrier abnormalities in DGAT2-deficient mice. The Journal of biological chemistry. 2004; 279:11767–11776. [PubMed: 14668353]

Sugihara K, Kitamura S, Yamada T, Ohta S, Yamashita K, Yasuda M, Fujii-Kuriyama Y. Aryl hydrocarbon receptor (AhR)-mediated induction of xanthine oxidase/xanthine dehydrogenase activity by 2,3,7,8-tetrachlorodibenzo-p-dioxin. Biochemical and biophysical research communications. 2001; 281:1093–1099. [PubMed: 11243847]

NIH-PA Author Manuscript

NIH-PA Author Manuscript

NIH-PA Author Manuscript

Sugimoto H, Okada K, Shoda J, Warabi E, Ishige K, Ueda T, Taguchi K, Yanagawa T, Nakahara A, Hyodo I, Ishii T, Yamamoto M. Deletion of nuclear factor-E2-related factor-2 leads to rapid onset and progression of nutritional steatohepatitis in mice. Am J Physiol Gastrointest Liver Physiol. 2010; 298:G283–G294. [PubMed: 19926817]

Tanaka T, Uchiumi T, Kohno K, Tomonari A, Nishio K, Saijo N, Kondo T, Kuwano M. Glutathione homeostasis in human hepatic cells: overexpression of gamma-glutamylcysteine synthetase gene in cell lines resistant to buthionine sulfoximine, an inhibitor of glutathione synthesis. Biochemical and biophysical research communications. 1998; 246:398–403. [PubMed: 9610371]

Tanaka Y, Aleksunes LM, Yeager RL, Gyamfi MA, Esterly N, Guo GL, Klaassen CD. NF-E2-related factor 2 inhibits lipid accumulation and oxidative stress in mice fed a high-fat diet. The Journal of pharmacology and experimental therapeutics. 2008; 325:655–664. [PubMed: 18281592]

Uno S, Dalton TP, Sinclair PR, Gorman N, Wang B, Smith AG, Miller ML, Shertzer HG, Nebert DW. Cyp1a1(−/−) male mice: protection against high-dose TCDD-induced lethality and wasting syndrome, and resistance to intrahepatocyte lipid accumulation and uroporphyria. Toxicology and applied pharmacology. 2004; 196:410–421. [PubMed: 15094312]

Verhulst SL, Nelen V, Hond ED, Koppen G, Beunckens C, Vael C, Schoeters G, Desager K. Intrauterine exposure to environmental pollutants and body mass index during the first 3 years of life. Environmental health perspectives. 2009; 117:122–126. [PubMed: 19165398]

Weisiger RA. Mechanisms of intracellular fatty acid transport: role of cytoplasmic-binding proteins. J Mol Neurosci. 2007; 33:42–44. [PubMed: 17901544]

Westerfeld WW, Richert DA. Liver and intestinal xanthine oxidases in relation to diet. The Journal of biological chemistry. 1951; 192:35–48. [PubMed: 14917648]

Westerfeld WW, Richert DA, Hilfinger MF. Studies on xanthine oxidase during carcinogenesis by p-dimethylaminoazobenzene. Cancer research. 1950; 10:486–494. [PubMed: 15434804]

Yang H, Magilnick N, Lee C, Kalmaz D, Ou X, Chan JY, Lu SC. Nrf1 and Nrf2 regulate rat glutamate-cysteine ligase catalytic subunit transcription indirectly via NF-kappaB and AP-1. Molecular and cellular biology. 2005; 25:5933–5946. [PubMed: 15988009]

Yeager RL, Reisman SA, Aleksunes LM, Klaassen CD. Introducing the "TCDD-inducible AhR-Nrf2 gene battery". Toxicol Sci. 2009; 111:238–246. [PubMed: 19474220]

Yoshinari K, Okino N, Sato T, Sugatani J, Miwa M. Induction of detoxifying enzymes in rodent white adipose tissue by aryl hydrocarbon receptor agonists and antioxidants. Drug metabolism and disposition: the biological fate of chemicals. 2006; 34:1081–1089. [PubMed: 16581946]

Yoshizawa K, Heatherly A, Malarkey DE, Walker NJ, Nyska A. A critical comparison of murine pathology and epidemiological data of TCDD, PCB126, and PeCDF. Toxicol Pathol. 2007; 35:865–879. [PubMed: 18098033]

Zender L, Hutker S, Liedtke C, Tillmann HL, Zender S, Mundt B, Waltemathe M, Gosling T, Flemming P, Malek NP, Trautwein C, Manns MP, Kuhnel F, Kubicka S. Caspase 8 small interfering RNA prevents acute liver failure in mice. Proceedings of the National Academy of Sciences of the United States of America. 2003; 100:7797–7802. [PubMed: 12810955]

Zhang YK, Yeager RL, Tanaka Y, Klaassen CD. Enhanced expression of Nrf2 in mice attenuates the fatty liver produced by a methionine- and choline-deficient diet. Toxicology and applied pharmacology. 2010; 245:326–334. [PubMed: 20350562]

NIH-PA Author Manuscript

NIH-PA Author Manuscript

NIH-PA Author Manuscript

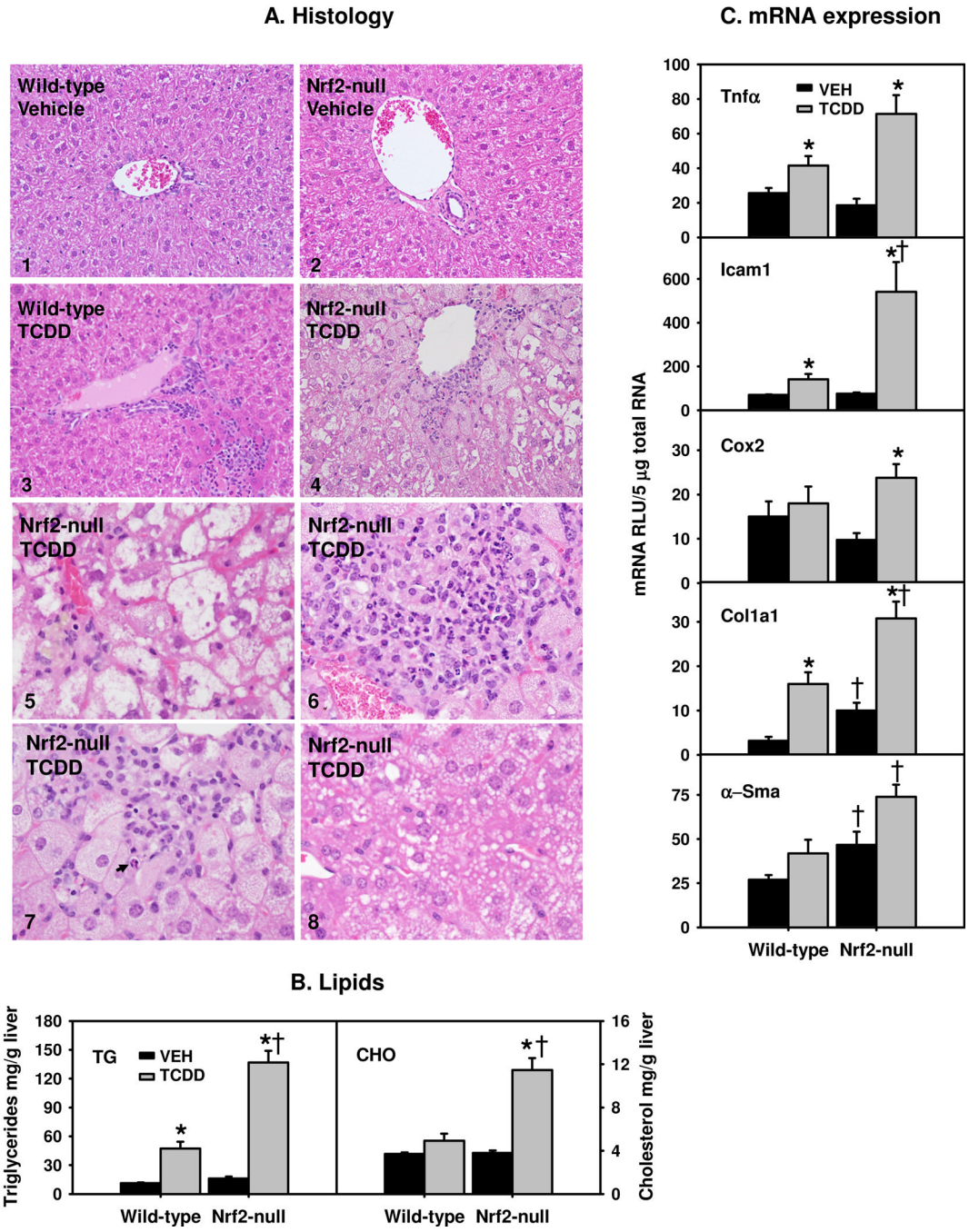

Fig. 1.

Steatohepatitis in TCDD-treated Nrf2-null mice. A1–4) Liver histopathology in vehicle (VEH)- and TCDD-treated wild-type and Nrf2-null mice. A5–8) Liver histopathology of TCDD-treated Nrf2-null mice showing ballooning degeneration (5), lobular inflammation (6), apoptosis (7, indicated by arrow) and microvesicular steatosis (8). H&E staining of paraffin embedded liver sections (5 µm and 400 × magnification). B) Hepatic levels of triglycerides (TG) and total cholesterol (CHO); and C) Hepatic mRNAs of inflammatory and fibrotic genes. Mean ± SE. N=4–5. * $p \leq 0.05$ versus corresponding vehicle-treated mice; † $p \leq 0.05$ versus corresponding wild-type mice.

NIH-PA Author Manuscript

NIH-PA Author Manuscript

NIH-PA Author Manuscript

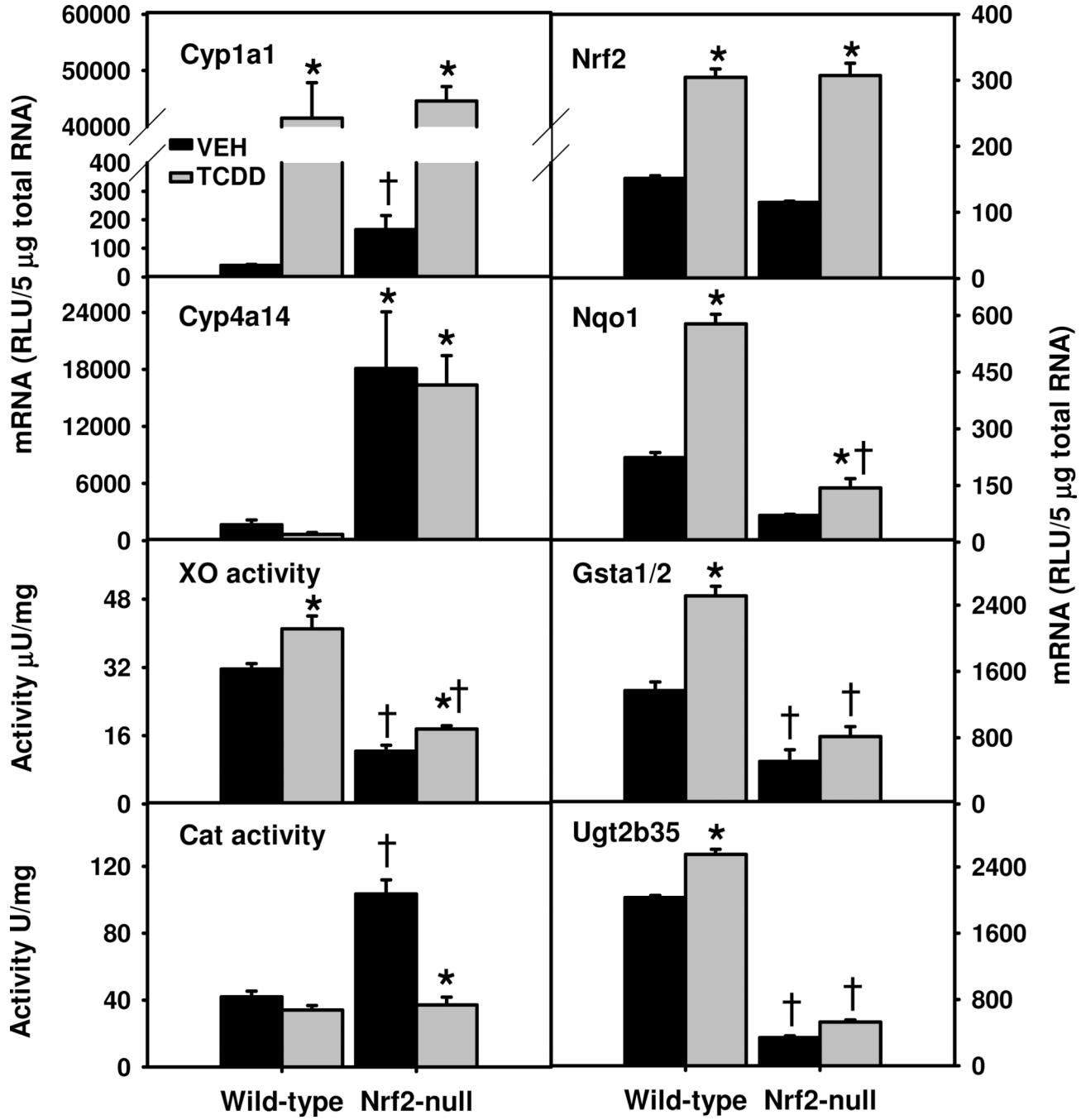

Fig. 2.

Hepatic mRNAs of AhR-target and redox genes (left panel) as well as Nrf2 and classical Nrf2-target Phase-II enzymes (right panel) in TCDD-treated Nrf2-null mice. Mean ± SE. N=4–5. * $p \leq 0.05$ versus corresponding vehicle-treated mice; † $p \leq 0.05$ versus corresponding wild-type mice.

NIH-PA Author Manuscript

NIH-PA Author Manuscript

NIH-PA Author Manuscript

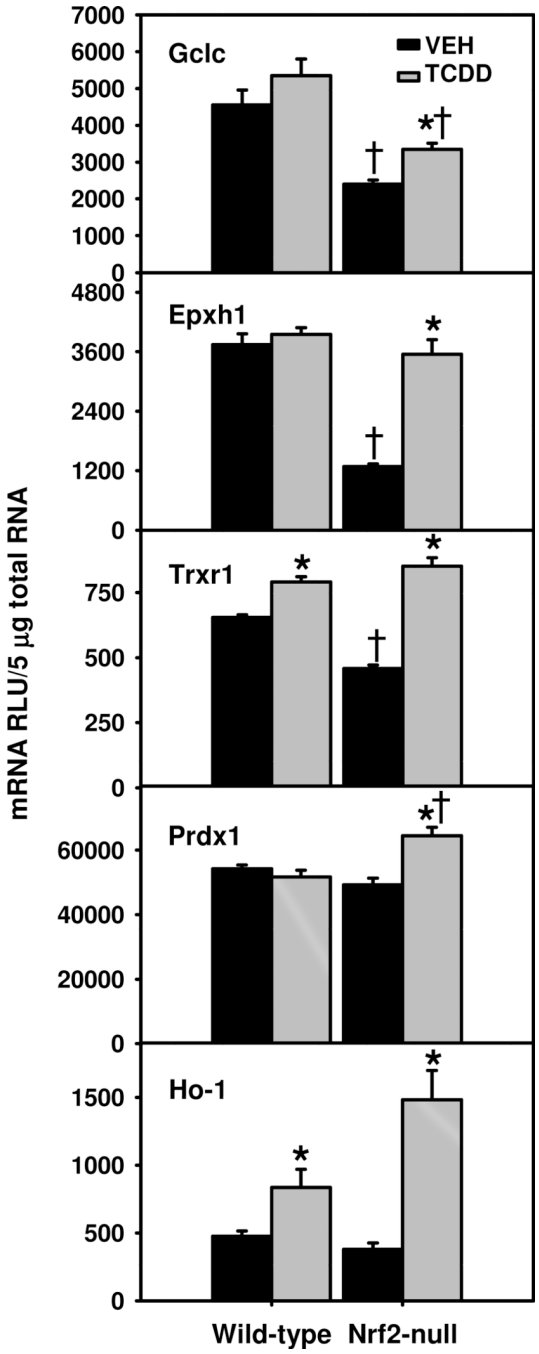

Fig. 3.

Hepatic mRNAs of Nrf2-target antioxidative genes in TCDD-treated Nrf2-null mice. Mean ± SE. N=4–5. * $p \leq 0.05$ versus corresponding vehicle-treated mice; † $p \leq 0.05$ versus corresponding wild-type mice.

NIH-PA Author Manuscript

NIH-PA Author Manuscript

NIH-PA Author Manuscript

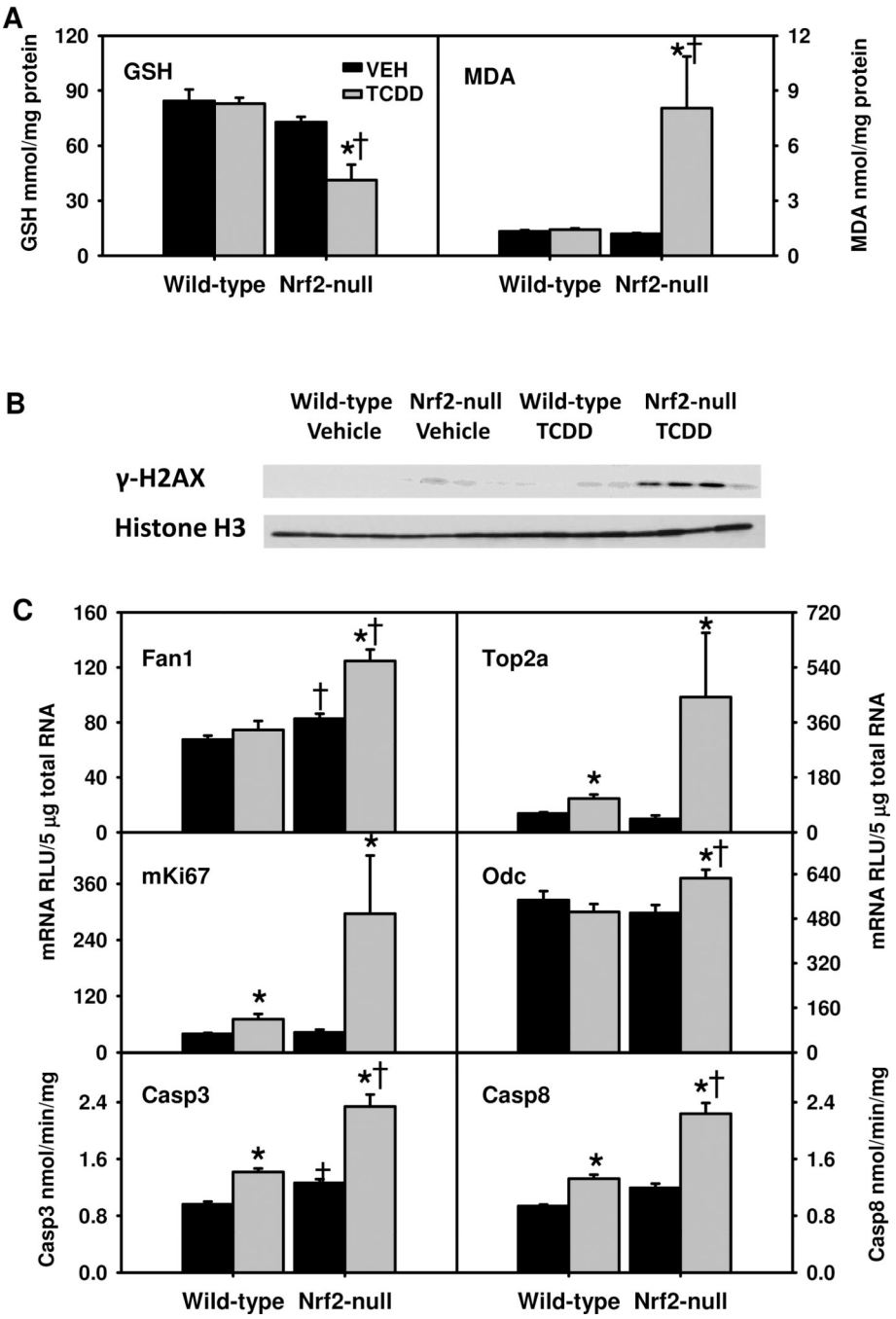

Fig. 4.

A) Hepatic levels of reduced glutathione (GSH) and malondialdehyde (MDA); B) hepatic protein levels of γ-H2AX; and C) hepatic mRNAs of DNA repair and proliferative genes as well as activities of caspase-3 (Casp3) and caspase-8 (Casp8) in TCDD-treated Nrf2-null mice. Mean ± SE. N=4–5. * $p \leq 0.05$ versus corresponding vehicle-treated mice; † $p \leq 0.05$ versus corresponding wild-type mice.

NIH-PA Author Manuscript

NIH-PA Author Manuscript

NIH-PA Author Manuscript

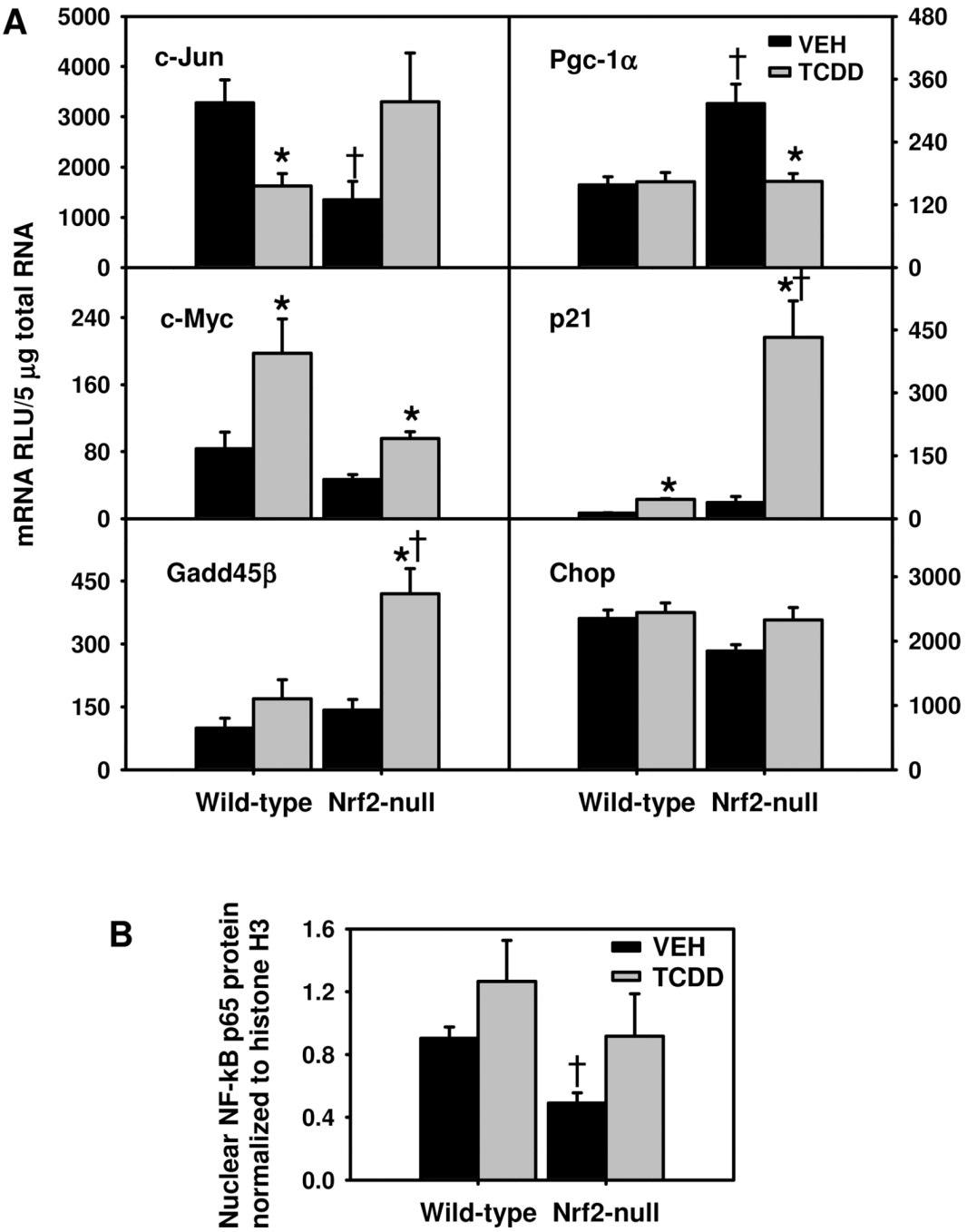

Fig. 5.

A) Hepatic mRNAs of transcriptional factors important in cell proliferation, apoptosis, and energy metabolism in TCDD-treated Nrf2-null mice; and B) Protein levels of NF-kB p65 subunit in nuclear extracts from livers of TCDD-treated Nrf2-null mice. Mean ± SE. N=4–5. * $p \leq 0.05$ versus corresponding vehicle-treated mice; † $p \leq 0.05$ versus corresponding wild-type mice.

NIH-PA Author Manuscript

NIH-PA Author Manuscript

NIH-PA Author Manuscript

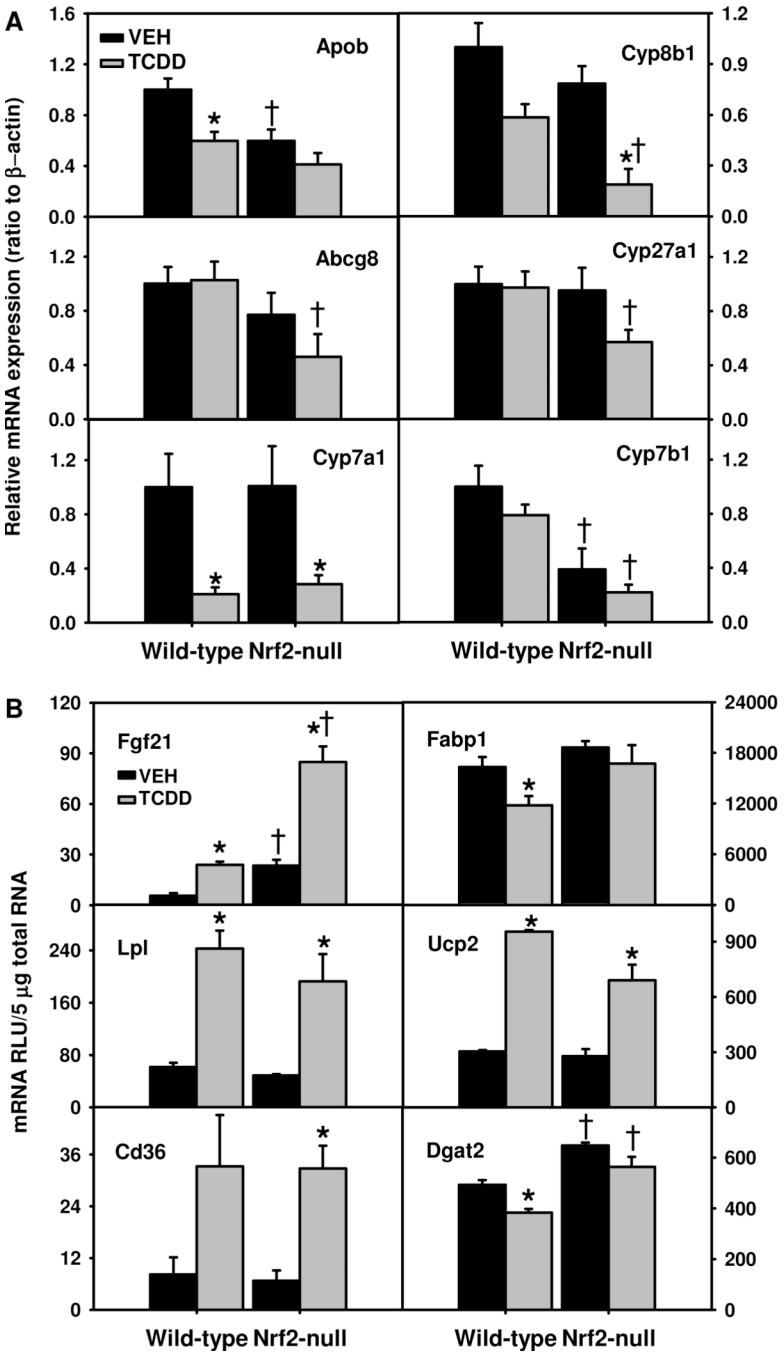

Fig. 6.

Hepatic mRNAs of genes important in cholesterol (A) and lipid (B) metabolism in TCDD-treated Nrf2-null mice. Mean ± SE. N=4–5. * $p \leq 0.05$ versus corresponding vehicle-treated mice; † $p \leq 0.05$ versus corresponding wild-type mice.

NIH-PA Author Manuscript

NIH-PA Author Manuscript

NIH-PA Author Manuscript

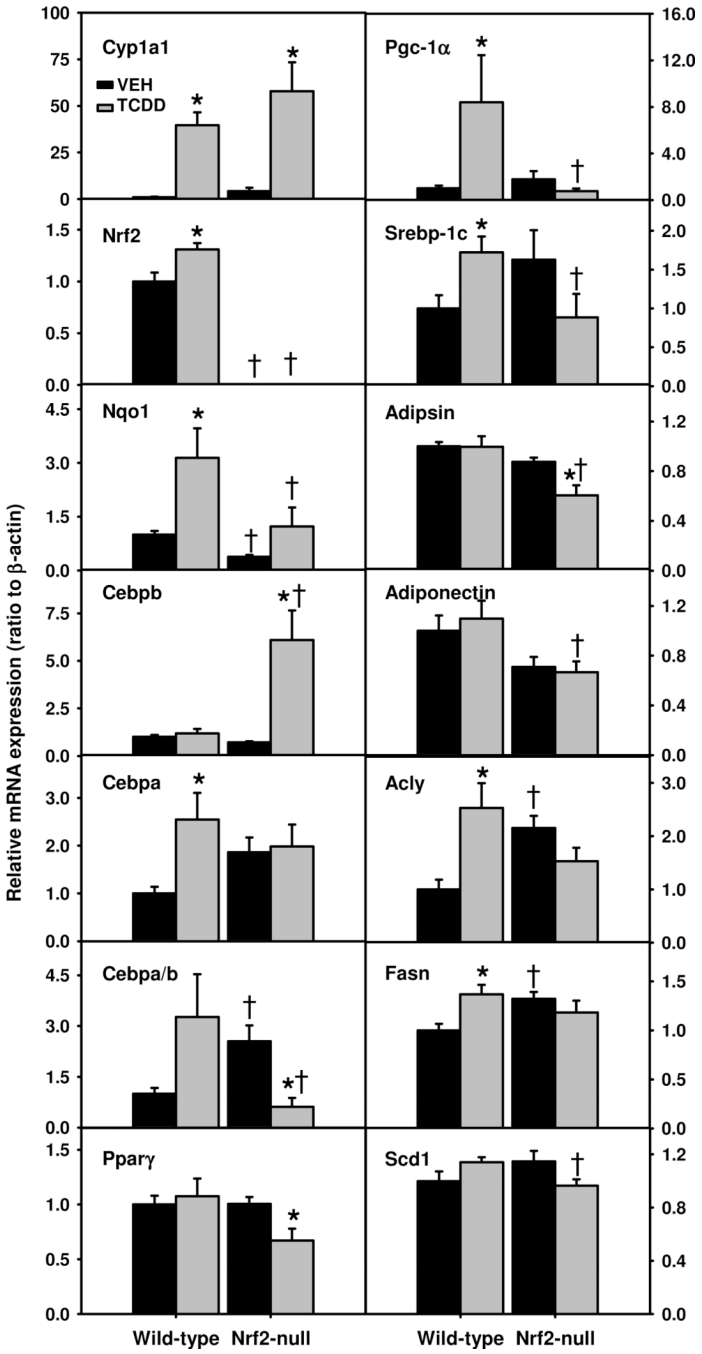

Fig. 7.

mRNAs of genes important in AhR and Nrf2 signaling as well as adipogenesis in epididymal white adipose tissue (WAT) of TCDD-treated Nrf2-null mice. Mean ± SE. N=4–5. * $p \leq 0.05$ versus corresponding vehicle-treated mice; † $p \leq 0.05$ versus corresponding wild-type mice.

NIH-PA Author Manuscript

NIH-PA Author Manuscript

NIH-PA Author Manuscript

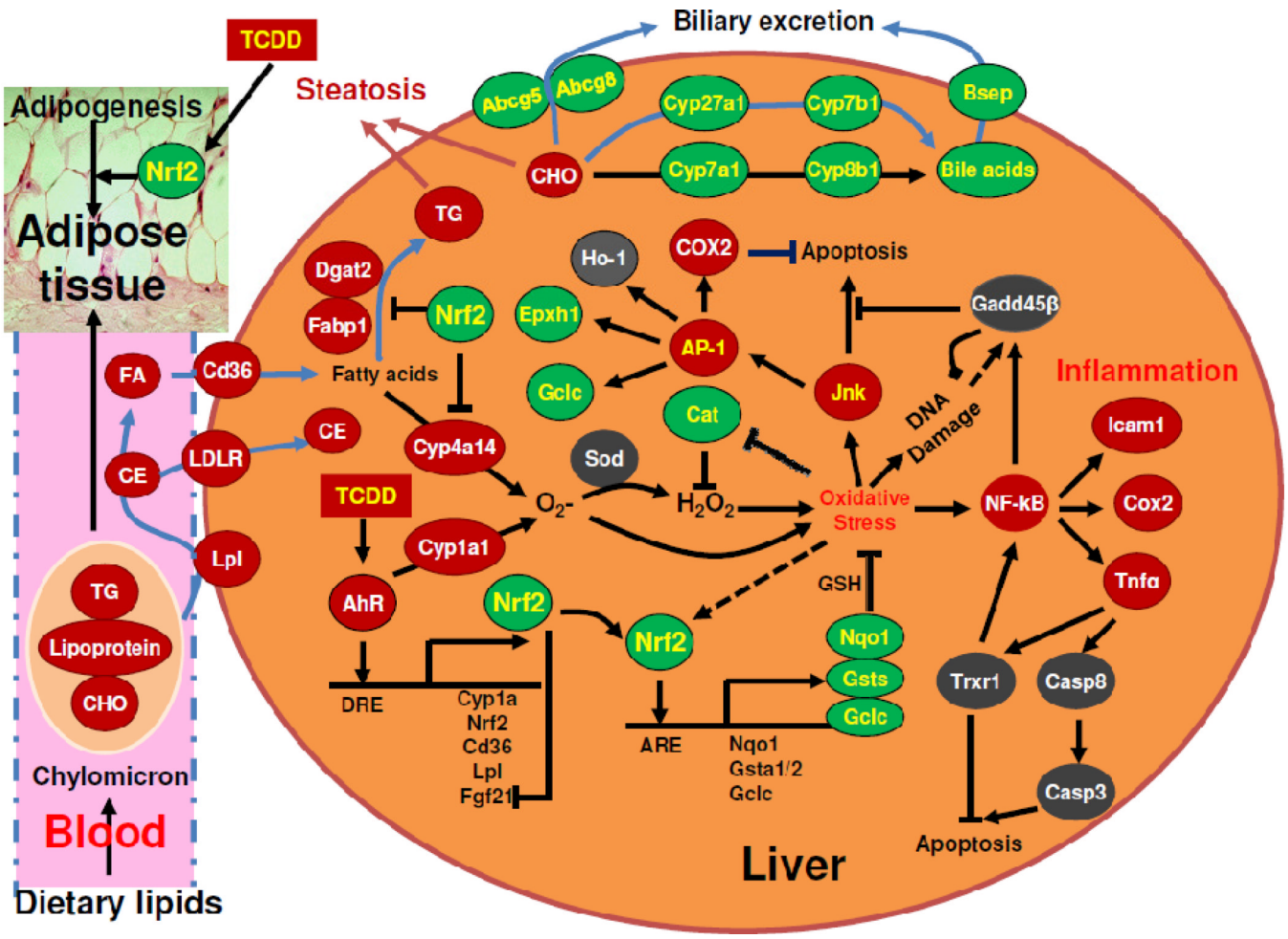

Fig. 8.

Diagram that summarizes the role of Nrf2 in protecting mouse liver against oxidative DNA damage and steatohepatitis induced by TCDD-mediated sustained activation of the AhR. TG, triglycerides; FA, fatty acids; CE, cholesteryl ester; CHO, cholesterol; DRE, dioxin response element; ARE, antioxidant response element.

NIH-PA Author Manuscript

NIH-PA Author Manuscript

NIH-PA Author Manuscript

Table 1

Alteration in body and tissue weights as well as blood chemistry in wild-type and Nrf2-null mice 21 d after TCDD treatment.

	Wild-type Vehicle	Wild-type TCDD	Nrf2-null Vehicle	Nrf2-null TCDD
Body weight before treatment (g)	**27.5 ± 1.2**	**26.6 ± 1.5**	**23.1 ± 2.6** *b*	**24.8 ± 1.7**
Body weight 21 d after treatment (g)	**28.6 ± 1.0**	**27.4 ± 1.5**	**23.3 ± 2.2** *b*	**24.3 ± 1.7** *b*
Body weight change (g)	1.2 ± 0.2	0.8 ± 0.4	0.2 ± 0.2 *b*	−0.6 ± 0.1 *a b*
Liver/body weight (g/100 g)	5.60 ± 0.09	6.72 ± 0.20 *a*	4.93 ± 0.24	6.08 ± 0.21 *a*
Kidney/body weight (g/100 g)	1.35 ± 0.02	1.31 ± 0.02	1.36 ± 0.05	1.35 ± 0.03
Spleen/body weight (g/100 g)	0.29 ± 0.004	0.36 ± 0.03	0.34 ± 0.02	0.27 ± 0.01
ALT (U/L)	16 ± 1	41 ± 6 *a*	18 ± 1	25 ± 11
ALP (U/L)	77 ± 3	85 ± 4	96 ± 5 *b*	124 ± 11 *b*
Triglycerides (mg/dl)	92.9 ± 4.6	92.9 ± 5.7	92.9 ± 4.3	97.8 ± 4.8
Cholesterol (mg/dl)	47 ± 2	36 ± 4 *a*	50 ± 2	37 ± 1 *a*
NEFA (mEq/L)	0.23 ± 0.03	0.24 ± 0.02	0.28 ± 0.02	0.26 ± 0.03

N=4–5, mean ± SE.

a $p \leq 0.05$ versus corresponding vehicle-treated mice.

b $p \leq 0.05$ versus corresponding wild-type mice.